# POLITECNICO DI TORINO

Collegio di Ingegneria Chimica e dei Materiali

**Corso di Laurea Magistrale**
**in Ingegneria Chimica e dei Processi Sostenibili**


Tesi di Laurea Magistrale

# Hybrid catalysts for the oxidation of biosourced furanic derivatives



**Relatori**

prof.ssa Stefania Specchia
prof. Erwann Guénin

**Candidato**

Enrico Antonuccio


Dicembre 2022

## Sommario

# I. Contesto

Il lavoro esposto in questa tesi è frutto di uno stage di ricerca effettuato presso i laboratori del dipartimento TIMR (transformations intégrées de la matière renouvelable) del centro di ricerca dell'UTC (Université de la technologie de Compiègne), tra marzo e luglio 2022, sotto la direzione del Professor Erwann Guénin e prende il titolo di "Catalyseurs hybrides pour l'oxydation de dérivés furaniques biosourcés".

Questo stage è stato svolto nell'ambito di un programma di mobilità internazionale Erasmus+ presso UTC della durata di due semestri accademici, iniziato ad agosto 2021 e conclusosi con la seguente ricerca, che originariamente è stata condotta in lingua francese, ma verrà dettagliata nel seguito dell'opera in inglese.

Il campo di ricerca su cui si sono concentrati gli esperimenti è stato attribuito e in ragione della filiera di Laurea Magistrale in ingegneria chimica in cui sono candidato, ovvero quella della sostenibilità di processi e prodotti dell'industria chimica e dell'ambito di lavoro del mio supervisore, direttore del dipartimento di trasformazione della materia rinnovabile dell'UTC.

Precedenti settori di investigazione scientifica del Prof. Guénin durante la sua carriera come docente di chimica all'UTC sono stati la sintesi di nanoparticelle metalliche per delle applicazioni in fototerapia, la caratterizzazione di nanoparticelle d'oro tramite molecole fosforate, lo sviluppo di processi di purificazione delle acque reflue tramite biocatalizzatori ibridi di fibroina della seta e l'ossidazione catalitica di molecole furaniche lignocellulosiche in prodotti chimici bio-derivati.
La trattazione dell'ossidazione di composti furanici derivanti dalla biomassa tramite catalisi ibrida di nanoparticelle d'oro in un idrogel di fibroina della seta risulta la sintesi di questi settori adattata ad una dimensione ecologica.

La vocazione ambientale della tesi giace infatti in due aspetti: da un lato la sintesi di unità costitutive monomeriche o "building blocks" di origine biologica e rinnovabile è cruciale per l'industria chimica per affrontare la sfida del rimpiazzo di materiali di origine fossile, come le plastiche e altri polimeri, e dall'altro la tecnologia che permette di arrivare a tale sintesi, ovvero la catalisi ibrida, riveste un ruolo chiave per la chimica verde.

Tale filosofia si articola nei canonici 12 principi della chimica verde, consultabili nell'appendice. Ma in particolare sono il settimo, il nono ed il decimo quelli più toccati.
In ordine, il settimo principio impone l'uso di materie prime rinnovabili nella sintesi organica ogniqualvolta sia tecnicamente ed economicamente possibile.

*"Le materie prime lignocellulosiche, come la biomassa forestale e i residui delle colture agricole, possono essere utilizzate per generare biocarburanti e prodotti biochimici. La conversione di questi materiali organici di scarto in prodotti biochimici è ampiamente considerata un approccio risolutivo per sviluppare una fonte di energia sostenibile, pulita e verde."* (Nadim Ayoub, 2022)

Al giorno d'oggi, la valorizzazione della biomassa lignocellulosica sta diventando una necessità per ridurre il ricorso alle risorse fossili; essa è particolarmente interessante perché fornisce un

accesso ai derivati del furano, che vantano molteplici applicazioni in ambito industriale non solo come biocarburanti, ma anche della chimica fine, in virtù dell'attività ottica conferita dal centro chirale presente nelle molecole.

Gli esperimenti condotti ricadono sotto quest'ottica in quanto sono stati finalizzati alla sintesi di una molecola target, l'FDCA, a partire da un suo precursore di natura lignocellulosica, l'HMF. Quest'ultimo è una molecola organica di formula $C_6H_3O$, rappresentata nell'immagine *I.I*

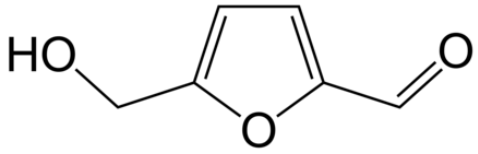


*Immagine I.I Struttura molecolare dell'HMF*

Esso deriva dall'idrolisi acido-catalizzata dei tre costituenti della biomassa forestale- cellulosa, emicellulosa e lignina- in glucidi a 5 o 6 atomi di carbonio, come fruttosio e glucosio, presenti nella cellulosa e nell'amido, che possono successivamente riformati tramite disidratazione per dare luogo a delle "molecole piattaforma". Infine, queste un ulteriore processo catalitico porta alla sintesi di una vasta gamma di chemicals e carburanti, ampiamente utilizzati in diversi campi e industrie. (Nadim Ayoub, 2022)**b**

Esiste un'ampia scelta di processi potenzialmente capaci di trasformare queste molecole piattaforma in carburanti e di funzionalizzarle. Nel caso dell'HMF, si opta tradizionalmente o per una riduzione a dioli oppure ad un'ossidazione in diacidi. Entrambe queste classi di molecole possono poi essere sfruttate per la sintesi di polimeri, possedendo due estremità funzionali. Le vie di sintesi e gli intermedi molecolari, sono visionabili nell'immagine *I.II* (Erwann Guénin, 2022)*:*

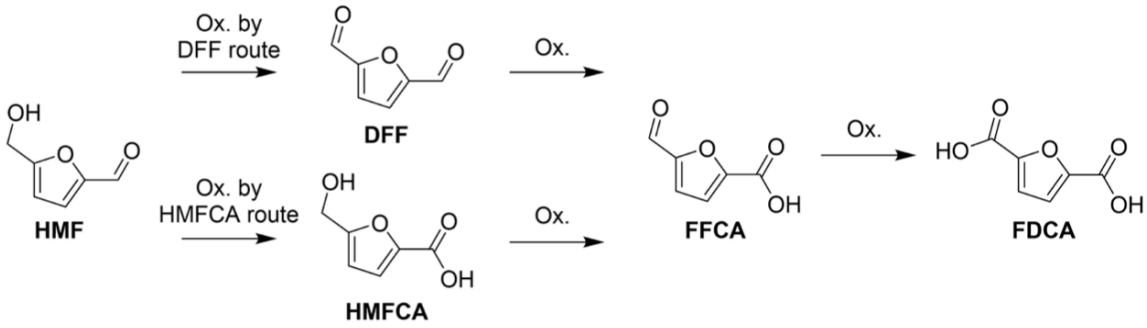


*Immagine I.II Percorso di reazione a stadi per ossidare l'HMF a FDCA*

In quest'ottica entra in gioco un altro principio della chimica verde, il nono, che prescrive l'uso indispensabile della catalisi.

*"I processi tradizionali di valorizzazione di queste molecole di origine biologica utilizzano la metallo-catalisi, di solito con metalli nobili, per ottenere buone conversioni, rese e selettività. Sebbene la catalisi sia uno dei pilastri della chimica verde, l'uso di metalli costosi, tossici e critici è spesso dannoso per questa denominazione. Di recente, quindi, la catalisi ibrida ha attirato l'attenzione di scienziati e ricercatori e tali catalizzatori possono essere considerati materiali catalitici verdi, perché possono essere altamente efficienti, facili da maneggiare, ecologici ed*

*economici in vari settori industriali. Questa dinamica è stata motivata dal desiderio di superare gli svantaggi della catalisi metallica e dagli interessi che si possono trarre dalla sua sostituzione."* (Nadim Ayoub, 2022)**c**

Nel fulcro dell'opera verrà presentata una metodologia di sintesi di un catalizzatore ibrido, definito *"la combinazione di materiali diversi che mostra proprietà amplificate rispetto ai componenti individuali. Può consistere di solo componenti inorganici o organici, ma sono decisamente di rilevante interesse quelli costituiti simultaneamente da entrambi, tra i quali si sviluppano dei veri e propri legami chimici e che esibiscono una struttura molecolare intrecciata altamente organizzata.*" (Kustov, 2021)

Gli esperimenti descritti nel seguito coinvolgono una dispersione di nanoparticelle d'oro in una matrice polimerica gelatinosa derivata dalla fibroina della seta. L'adoperare una biomolecola come la fibroina per dare luogo alla struttura del catalizzatore permette di riagganciarsi all'ultimo dei principi invocati, il decimo, che predilige la progettazione di prodotti biodegradabili, riducibili a sostanze chimiche innocue dopo il loro utilizzo.

Lo scopo della tesi è da un lato eseguire e migliorare il protocollo di estrazione della fibroina dalla seta, come messo a punto da Rockwood et al., finalizzato alla sua trasformazione in idrogel, per accogliere le nanoparticelle catalitiche appositamente sintetizzate, e dall'altro quello di caratterizzare il catalizzatore ibrido ottenuto.
A tale scopo si farà ricorso a tutta una serie di tecniche analitiche fisicochimiche, come la microscopia elettronica a trasmissione e a scansione e la dispersione dinamica della luce, che verranno dettagliate nel corso dell'opera. Inoltre, occorrerà testare il biocatalizzatore nella reazione target di ossidazione dell'HMF in FDCA. Per fare ciò si effettuerà un'ossidazione preventiva della molecola tramite una via classica metallo catalizzata, già esistente nella letteratura, come quella proposta da Miediziak et al., che fungerà da secondo termine di paragone, così da confrontare le performance del catalizzatore ibrido specificamente progettato rispetto alla metodologia precedente.

# II. Nanoparticelle metalliche

Limitatamente alla sua componente inorganica, si è scelto di sperimentare l'oro come metallo del catalizzatore. In particolare, è stata preparato in forma di nanomateriale, cioè di particelle solide di dimensione inferiore ai 100 nm. Quest'ultime sono state adoperate come dispersione colloidale in fase acquosa, venendo così a formare un sol.
La riduzione alla scala nanometrica conferisce intriganti proprietà chimico-fisiche al metallo, quali la duttilità, conduttività ed elasticità. Questo metallo eclettico è oggetto di studio nei campi della catalisi, come della fototerapia termica e della biosensoristica.
L'origine di queste proprietà discende proprio dalla taglia nanoscopica delle particelle dorate, che secondo diversi ne accentua moltissimo il potere catalitico, inoltre il conveniente rapporto superficie/volume permette di economizzare sulla terra rara, con un beneficio doppiamente economico e ambientale.
Tipicamente le reazioni catalizzate sono l'ossidazione e la riduzione; recentemente si stanno sviluppando delle tecnologie volte ad associare le nanoparticelle ad un'azione enzimatica, per formare dei 'nanozimi', capaci di riprodurre le capacità di un dato enzima e di, grazie all'inclusione della proteina sul metallo, ingigantirne il potenziale catalitico.

### Materiali e metodi

Il protocollo adottato per la sintesi delle nanoparticelle prevede un approccio detto <<bottom-up>>, cioè basato sull'assemblaggio chimico di atomi provenienti da molecole differenti al fine di formare degli aggregati nanometrici, a differenza dell'alternativa <<top-down>>, che prevede di decomporre il materiale massivo in forma elementare fino alla taglia di nanoparticelle con le dovute tecniche fisico-meccaniche.

La molecola di partenza è l'acido cloroaurico triidrato, di formula molecolare $HAuCl_4 \bullet 3H_2O$, sottoforma di solido granulare giallastro, in cui l'oro è presente nel suo stato di ossidazione +III. Per poterlo convertire allo stato elementare, caratterizzato dunque da un numero di ossidazione uguale a zero, è necessario in primis ridurlo chimicamente, ed in secundis di un agente chelante che possa favorire l'aggregazione degli atomi a formare le nanoparticelle di taglia controllata in mezzo acquoso.
"Esistono attualmente molteplici modalità di sintetizzare delle nanoparticelle d'oro e si tenterà di mostrare il principio discriminante sulla base del reagente messo in gioco. Se il complesso precursore più utilizzato è l'acido tetracloroaurico, le sintesi si differenziano per la natura degli agenti riducenti e dei ligandi introdotti. Si distinguono grossolanamente due categorie di sintesi:

- Le sintesi dove il composto riduttore è anche il ligando; è soprattutto il caso della sintesi di <<Turkevich>>. Il ligando, generalmente introdotto in eccesso partecipa al processo di ossido-riduzione del complesso d'oro e ne stabilizza i nanocristalli formati
- Le sintesi facenti intervenire un riduttore ed un ligando ben distinti"

(Aufare, 2016)

Come esposto da Aufare, il crescente tentativo di valorizzare la biomassa, pilastro della chimica verde, porta a trovare dei reagenti per le vie di sintesi tra le molecole naturali, come implicitamente prescritto dai principi III, VII e X.
Nel corso degli esperimenti condotti in questa sede, ci si è focalizzati sull'uso degli HMBP (idrossimetilbifosfonati) per la sintesi e funzionalizzazione delle nanoparticelle d'oro. Tali composti, essendo caricati negativamente, sono degli ottimi ligandi per stabilizzare efficacemente le nanoparticelle d'oro.

Il protocollo della reazione, in maniera analoga alla reazione di Turkevich, prevede di mescolare in una fiala

- 10 mL di acqua distillata
- 250 μL di una soluzione a PH 8,2 di un HMBP
- 125 μL di una soluzione di acido cloaurico a concentrazione 0,25 mM (come in foto II.I)

*Foto II.I soluzione di acido cloroaurico impiegata per la sintesi delle NP*

Dal momento che in partenza le soluzioni di HMBP hanno un PH acido, è stata aggiunta una soluzione concentrata di NaOH per ripristinare la basicità al valore necessario.
In seguito, la reazione è avvenuta mescolando i due reagenti all'interno di una fiala successivamente posta all'interno di un apposito reattore a microonde provvisto di agitatore magnetico per 30 minuti, di cui i primi 25 a 100°C ed i restanti a 45°C. Questa metodica introduce una novità rispetto alla sintesi di Turkevich per quanto riguarda il modo di fornire il calore necessario: al posto dei classici vettori come convezione e conduzione, che ne causano una ripartizione eterogenea all'interno del volume, il reattore a microonde garantisce performances efficacissime, permettendo di scaldare il sistema a 100 °C in pochi secondi. Le microonde sono caratterizzate da una lunghezza d'onda compresa tra 1cm e 1m, perciò ad esse è associata un'energia abbastanza debole in accordo alla legge di Planck:

$$E = hc/\lambda$$

Tale proprietà le impedisce di rompere dei legami chimici e cambiare l'identità di una molecola, ma solo di mettere in rotazione i dipoli presente o di provocare la conduzione ionica. Attraversando il vetro trasparente ad esse, mettono in oscillazione gli ioni e le molecole dipolari presenti nella soluzione, in funzione della sua costante dielettrica, molto elevata nel caso dell'acqua. Questi collidendo tra di loro dissipano energia e riscaldano uniformemente il sistema.

Diverse tecniche analitiche sono state adoperate per caratterizzare le soluzioni di nanoparticelle ottenute, volte principalmente a conoscere la taglia di esse, o un ventaglio di suoi valori. Si tratta della microscopia elettronica a trasmissione (TEM) e della diffusione dinamica della luce (DLS), i cui principi di funzionamento e dispositivi impiegati vengono descritti nei paragrafi 3.1 e 3.3 dell'opera.
Anche i risultati ottenuti per mezzo delle tecniche in questione sono espressi e commentati nel dettaglio nel capitolo loro dedicato.

## III. La fibroina della seta

“La seta gode della reputazione di ‘regina delle fibre naturali’, in virtù delle sue uniche qualità, come la resistenza, la finezza e la dolcezza al tatto.” (Basu, 2015)

La seta viene ottenuta dai bozzoli di diversi bachi, noti come “*Bombyx mori*”. Si tratta della versione domestica del baco da seta, che a differenza del suo lontano parente selvatico, “*Bombyx mandarina*”, dipende in tutto e per tutto dall’attività umana. Non è infatti in grado di volare, capacità necessaria per l’accoppiamento, e scappare dai predatori. Inoltre, a causa del suo albinismo, non dispone di alcuna abilità mimetica, diventando una facile preda. Per contro, in seguito alla domesticazione, B. mori ha sviluppato dimensioni notevoli, come visibile nell’immagine III.I- tratta da Papilionea (Tognon, 2022) con modifiche- e adattato la sua capacità digestiva alla sua alimentazione ininterrotta.

*Immagine III.I Femmina di una falena di Bombyx mori appena uscita dal bozzolo*

Per via della domesticazione B. mori raggiunge dimensioni maggiori rispetto a B. mandarina, ed inoltre mostra un notevole appetito: mangia foglie di gelso bianco giorno e notte, senza interruzione, e di conseguenza crescono rapidamente, a tale scopo ha finanche migliorato la sua capacità digestiva. Il loro pasto è interrotto solo quattro volte, le "dormite", in corrispondenza di altrettante mute.
Quando la testa della larva diviene più scura indica che sta per avvenire la muta, durante la quale l’animale non si alimenta e cambia il suo involucro esterno, perché il corpo della larva cresce nel tempo; pertanto, l’involucro deve essere adattato alle maggiori dimensioni. Terminate le quattro mute il corpo della larva diviene leggermente giallo e si prepara ad entrare nello stato di pupa costruendo attorno a sé un bozzolo di seta secreta dalle ghiandole salivari. Prima della filatura del bozzolo la larva deve eliminare tutti i liquidi in eccesso e le feci che non possono essere contenute nel bozzolo, questo momento viene definito dagli allevatori "purga". La bava sottilissima a contatto con l'aria si solidifica e, guidata con movimenti ad otto della testa, si dispone in una trentina di strati concentrici formando un bozzolo di seta grezza, costituito da un singolo filo continuo di seta di lunghezza variabile fra i 300 e i 900 metri.

All’interno del bozzolo avviene l’ultima muta che porta B. mori dallo stadio larvale a quello di pupa. Dopo circa due settimane all’interno del bozzolo, la pupa metamorfosa in farfalla e secerne degli enzimi che creano un buco nel bozzolo che le permettono di fuoriuscire, rendendo il filo di seta che lo compone inutilizzabile. Di conseguenza, gli allevatori uccidono le crisalidi in appositi essiccatoi prima che questo avvenga. L'immersione in acqua bollente permette il dipanamento del filo di seta sciogliendo parzialmente lo strato proteico di sericina che avvolge il filo di seta. In alcune culture, la crisalide, estratta dal bozzolo, viene mangiata.
Alcuni bozzoli vengono risparmiati per consentire la riproduzione del baco.
In base al ciclo vitale il baco da seta domestico è suddiviso in tre gruppi. In Europa è stato prevalentemente utilizzato il baco con un solo ciclo di riproduzione all’anno, le uova infatti vanno in ibernazione durante l’inverno e si schiudono in primavera. In Cina, Giappone e Corea si trova il baco con due cicli di riproduzione all’anno, e ultimo ma non meno degno di nota, il baco con più di due cicli all’anno che si trova solo ai tropici.
(Begher, 2022)

Le fibre della seta, nonostante il basso modulo di Young, sono uno dei materiali naturali più resistenti (basti pensare alla tensione di rottura pari a 740 MPa), e questo grazie alla sua struttura molecolare. I filamenti della seta sono costituiti da due proteine: la fibroina (70%) e la sericina (30%). La prima, caratterizzata da una catena idrofoba, costituisce il nucleo del filamento, rivestita esternamente dalla seconda, affine all’acqua e dalla consistenza vischiosa. Per l’industria tessile e le notevoli applicazioni biotecnologiche, la fibroina è oggetto di interesse scientifico. Se ne conosce la composizione biochimica della catena polimerica: glicina (45%), alanina (29%) e serina (12%), con tracce di altri amminoacidi come triptofano, valina e tirosina. Quando questi si trovano nella loro struttura primaria, cioè di semplice scheletro polipeptidico, si arrangiano in due catene, una più pesante (390 kDa) ed una più leggera (26 kDa), tenute insieme grazie ai ponti disolfuro tra due cisteine. Inoltre, lo scarso ingombro sterico della glicina, il più piccolo degli amminoacidi, permette l’avvicinamento delle catene e l’irrobustirsi dei legami secondari che le congiungono, da cui discendono l’elevata robustezza del tessuto. Infine, data la sua origine naturale, la seta è biocompatibile e biodegradabile e ciò ne permette numerose negli ambiti della medicina e dell’ecologia.
Tra queste si reputa di particolare interesse la formazione di un idrogel contenente delle nanoparticelle per dotarlo di una funzione specifica. In particolare, quando delle particelle metalliche sono ottenute in soluzione acquosa attraverso un ligando biocompatibile, quest’ultimo assume un ruolo importante per la loro dispersione nella matrice gelatinosa, senza inficiarne i consueti meccanismi di gelificazione e comportamento reologico, ma arricchendola con nuove proprietà chimico-fisiche. (Marin, 2021)

Dal momento che la preparazione del gel richiede l’uso della fibroina pura, per metterla in atto è propedeutico il processo di estrazione della proteina, che consiste nel trasformare la materia prima grezza, cioè i bozzoli del B. mori privati della crisalide, in una soluzione acquosadella stessa. L’immagine al microscopio elettronico delle fibre è mostrata nell’*immagine III.I,* tratta da “fibroina di seta” con modifiche:

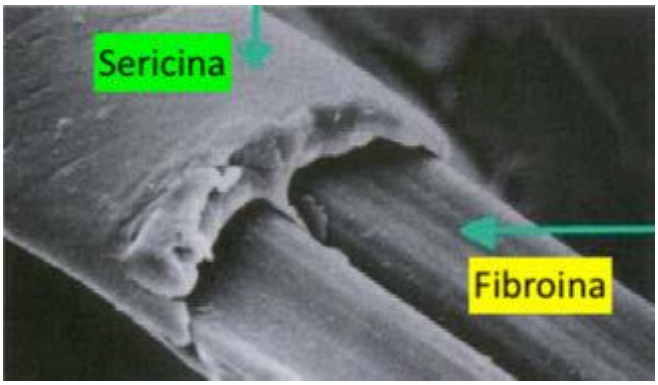


*Immagine III.II Struttura di una fibra di seta vista al TEM; in evidenza le due proteine costituenti*

(Anon., 2022)

Il processo consta di quattro operazioni consecutive, messe in atto e canonizzate per prima da Rockwood et al.:

i. Processo di 'degumming', ovvero di rimozione dello strato esterno di sericina dal filamento, per mezzo della differente affinità della proteina con solventi idrofili. Il processo viene eseguito in acqua bollente in cui è disciolto del $NaCO_3$ per una durata controllata; la taglia media in termini di PM della fibroina ottenuta dipenderà dalla durata di questo lasso di tempo, scelto intorno ai trenta minuti. Una volta trasferita la componente solubile nel mezzo aquoso, la fibroina è recuperata come un batuffolo indisciolto, che deve essere ben sciacquato e strizzato per purificarla dai resti salini.

ii. Processo di dissoluzione della fibroina tramite LiBr; l'effetto del sale è di rompere i legami disolfuro che tengono insieme la proteina, così da renderla temporaneamente solubile in acqua. Il processo viene effettuato all'interno di un'autoclave riscaldante per diverse ore. Alla fine si ottiene una soluzione viscosa e appiccicosa di colore giallino, la quale può essere aspirata e iniettata tramite una siringa.

iii. Dialisi della soluzione; lo scopo è di rimuovere dalla soluzione di fibroina il sale di LiBr precedentemente aggiunto tramite una dialisi in acqua distillata. Il principio di funzionamento è la diffusione del soluto dalla soluzione iniettata quando è ancora calda all'interno di un'apposita membrana porosa semipermeabile; da quest'ultima il sale può diffondere nel bagno acquoso circostante grazie alla taglia dei pori, invece la fibroina ne resta intrappolata all'interno. La dialisi viene condotta per tre giorni consecutivi, ricambiando l'acqua frequentemente.

iv. Centrifugazione della soluzione; due stadi di centrifugazione per 20 minuti a 9000 rpm intervallati da un travaso permettono di separare le impurità precipitate e chiarificare la soluzione.

(Danielle Rockwood, 2011)

# IV. La formazione degli idrogel

Gli idrogel sono strutture tridimensionali in grado di assorbire grandi quantità di acqua. In genere, gli idrogel non si dissolvono grazie alla fitta rete legami chimici o fisici e/o di aggrovigliamenti di catene. Esistono in natura sotto forma di reti di polimeri come il collagene o la gelatina, oppure possono essere prodotti sinteticamente.

La capacità degli idrogel di assorbire e trattenere un grande volume di liquidi li rende interessanti per scopi di disinquinamento, in particolare nel contesto dell'eliminazione di sostanze pericolose presenti nell'ambiente. Gli idrogel sensibili all'ambiente possono servire per un'ampia varietà di applicazioni grazie alla loro capacità di rispondere ai cambiamenti ambientali, in genere mostrando variazioni di volume. Gli stimoli tradizionali che provocano la risposta degli idrogel sono il pH, la temperatura e la forza ionica. Anche gli analiti e i biomarcatori, tra cui il glucosio, le proteine e il DNA, provocano la risposta degli idrogel. Grazie all'ampia varietà di stimoli di risposta, gli idrogel possono essere incorporati in sensori o attuatori, o essere utilizzati in sistemi di somministrazione controllata di farmaci, biosensori, impalcature per l'ingegneria tissutale, organi artificiali, bendaggi per la guarigione delle ferite, membrane fisiologiche, lenti a contatto e valvole microfluidiche. **(N.A. Peppas, 2012), (Rei, 2021)**

La gelificazione è un processo importante per un'ampia gamma di applicazioni in campo alimentare, farmaceutico e delle scienze dei materiali. Una caratteristica comune a tutte le reazioni di gelificazione delle proteine è che richiedono una transizione strutturale iniziale che può essere considerata come una trasformazione da una struttura non reattiva a una reattiva che aumenta la probabilità di interazioni intermolecolari**. (Erik van der Linden, 2009)**

La gelificazione è stata descritta come l'associazione o la reticolazione di lunghe catene polimeriche per formare una rete continua tridimensionale che intrappola e immobilizza il liquido al suo interno per formare una struttura cristallina estremamente viscosa più grande di quella iniziale.
I principali costituenti responsabili della gelificazione sono colloidi di carboidrati e proteine. Pertanto, più l'idrogel è concentrato in proteine, più gli idrogel formati sono resistenti alla compressione e alla deformazione. Ciò è dovuto a una rete molecolare più compatta che consente una migliore distribuzione delle sollecitazioni.

I meccanismi di gelificazione rimangono poco conosciuti. I meccanismi coinvolti nella formazione del gel per le proteine sono complessi e possono coinvolgere i legami salini tra i gruppi amminici e carbossilici della catena laterale, i legami idrogeno tra i peptidi e i legami incrociati disolfuro. La maggior parte dei carboidrati richiede invece il calore per la gelificazione (ad esempio, la pectina); si ritiene che questo fornisca energia per alterare la struttura della molecola, rendendola più adatta alla reticolazione. Spesso sono necessari ioni specifici per completare il processo di gelificazione; inoltre, la rete di gel può ridursi durante la conservazione, liberando acqua libera; questo processo è noto come pianto o sineresi.
I fattori coinvolti nella gelificazione sono la formazione di catene casuali e la reticolazione delle catene, tramite legami idrogeno o ponti salini. Alcuni gel sono chiari e reversibili termicamente, come la gelatina; altri sono torbidi o opachi, come l'albume d'uovo.

La capacità di gelificazione della maggior parte delle proteine è influenzata dal pH, dalla temperatura, dal grado di rigonfiamento, dall'ambiente ionico e dalla presenza di altre sostanze.
La gelificazione può essere misurata in due modi. Il primo consiste nel misurare il tempo in cui una soluzione del materiale forma un gel quando viene riscaldata a temperatura costante. Per le proteine, la concentrazione utilizzata è compresa tra l'8% e il 12% e le temperature tra 80 °C e 140 °C. Il secondo metodo prevede la misurazione di alcune proprietà reologiche del gel, come la resistenza, la durezza o la comprimibilità. **(Lewis, 1996)**

### Gelificazione chimica

I protocolli presentati in letteratura per controllare la formazione e le caratteristiche degli idrogel descrivono due tecniche principali: la gelificazione fisica e quella chimica. La gelificazione fisica può essere indotta applicando una forza fisica e si basa sulla formazione di legami non covalenti tra le catene di SF. Tuttavia, non sarà trattata in questo studio perché ci concentriamo sulla gelificazione chimica. Questa è causata dalla formazione di legami covalenti in presenza di un enzima, di un catalizzatore chimico o di un'altra specie chimica.
Siamo particolarmente interessati alla reticolazione assistita da enzimi per la sua bassa tossicità. Inoltre, le reazioni enzimatiche catalizzate sono molto specifiche e consentono un buon controllo del prodotto ottenuto.

D'altra parte, l'immobilizzazione degli enzimi su un supporto, come un idrogel, consente una maggiore stabilità dell'enzima. Questo preserva la sua attività e la sua struttura funzionale perché è fisicamente intrappolato in una matrice ospite, in questo caso la rete polimerica di fibroina che costituisce l'idrogel. **(Rei, 2021)**

In questo studio, l'idrogel in questione è costituito da SF sintetizzato in precedenza e da un enzima. Due tentativi di gelificazione sono riportati nell'opera, rispettivamente adoperando due enzimi di natura diversa (Laccasi e HRP) e due protocolli adattati al diverso funzionamento dei due, come consultabile al paragrafo 5.2. Per quanto riguarda l'incorporazione della soluzione NP, in un primo tentativo si è scelto di sostituirla con acqua, perché l'obiettivo era quello di testare l'efficacia del gel.

## V. La reazione di ossidazione

Come anticipato nel primo capitolo, il cuore della ricerca è costituito dalla reazione di ossidazione del reagente chiave, l'HRP, nel prodotto target FDCA.
In seno a questo processo, il catalizzatore ibrido, dato dall'idrogel di fibroina arricchito delle nanoparticelle sintetizzate ad hoc, trova la sua principale applicazione.
Tuttavia al fine di testare questa reazione è necessario avere un quadro di riferimento, così da comparare l'efficacia di questo catalizzatore e stabilire se la sinergia tra enzima e catalisi metallica ne giustifica la sofisticata via di sintesi.

A tale scopo nei paragrafi 6.2 e 6.3 sono dapprima sintetizzati dei protocolli di reazione di ossidazione analoghe a quella ricercata, ma senza l'ausilio della componente enzimatica, e successivamente viene riportata l'analisi dei risultati ottenuti implementando nella realtà di laboratorio tale protocollo tramite cromatografia su strato sottile.

# VI. Conclusioni

Il lavoro sperimentale condotto presso i laboratori di UTC accompagnato dalla ricerca bibliografica qui riassunta, e più esaurientemente presentata nella sezione successiva dell'opera, è stato volto alla sintesi di un catalizzatore ibrido per l'ossidazione e funzionalizzazione di molecole furaniche derivanti dalla biomassa.
Tuttavia, ogni singola parte degli esperimenti ha una sua individuale utilità; è dunque possibile individuare accanto all'obiettivo generale che ha indirizzato lo stage di ricerca, conferendogli la sua organicità, tutta una serie di 'tasks' che sono stati esplorati per raggiungerlo. Ad ognuno di essi sarà dedicato un capitolo dell'opera.
Tra questi è possibile annoverare: la sintesi e caratterizzazione delle nanoparticelle d'oro, l'estrazione della fibroina dalla seta, la sua gelificazione e il test sull'ossidazione dell'HMF.
Queste microaree di interesse scientifico hanno permesso di cogliere dei frutti in senso assoluto.
La formazione delle nanoparticelle metalliche è stata indubbiamente la parte più fervida dell'esperienza.
Grazie alla sintesi con il reattore a microonde si è ottenuta una dispersione omogenea di particelle della taglia desiderata, intorno ai 20 nm di diametro; questo successo dovuto alla via di sintesi effettuata da Aufare, ci permette di avvallare le sue sostanziali modifiche rispetto alla pregressa sintesi di Turkevich.
Le tecniche analitiche per caratterizzare la dispersione sono doppiamente utili: e per l'intrinseca ispezione qualitativa e quantitativa delle nanoparticelle e per farmi approcciare ai sofisticati dispositivi di laboratorio adoperati per condurle. Nonostante per ogni analisi microscopica ci sia stato un operatore professionale responsabile di effettuarla, allo scopo di comprendere il principio di funzionamento dell'apparecchio e interpretarne correttamente i risultati, sono stato sottoposto ad una specifica formazione. Nel corso dell'opera verranno riportati i punti cardine di ogni tecnica al momento del suo utilizzo, arricchiti di una documentazione sitografia.

La sezione più spinosa del lavoro è stata l'estrazione della fibroina. Nonostante il procedimento applicato fosse già stato collaudato, un numero di variabili possono intervenire nel processo in ogni singolo passaggio, inficiando il risultato finale e rendendo necessario ricominciare da capo. Nel paragrafo 4.3 "Troubleshoots" è presente un excursus su tutti gli aspetti che meritano di essere particolarmente attenzionati perché fonti di rischio. Data la soddisfacente qualità di soluzione ottenuta seguendo il protocollo Rockwood, si può concludere che questo sia uno dei migliori nel panorama attuale; tuttavia, la pratica svolta e soprattutto i numerosi incidenti riscontrati permettono di apportare qualche miglioria che si cercherà di riassumere di seguito.
La durata della fase di degumming può essere incrementata di 10 minuti; grazie a questo tempo supplementare i bozzoli ormai deprivati della sericina hanno la possibilità di intrecciarsi in un unico batuffolo di fibroina e anche la fase acquosa acquisirà una colorazione più torbida, indice dell'aumento in concentrazione di sericina che si trasferisce nel solvente.
Al momento dell'iniezione della fibroina nelle cassette per dialisi è consigliabile aggiungere dell'acqua distillata per fluidificare la soluzione; infatti, raffreddandosi durante il processo, la sua viscosità tenderà ad aumentare, rendendo più difficoltoso farla fluire attraverso il foro della siringa. Tale quantitativo d'acqua deve essere misurato e tenuto in conto al momento

del calcolo della concentrazione in fibroina della soluzione e non deve essere tale da fare scendere tale valore al di sotto del 4%.
Il passaggio della dialisi costituisce la cartina di tornasole del procedimento: è in questa fase che si vedrà se il processo darà dei buoni frutti o la soluzione è difettosa. Nel corso della pratica sperimentale, data l'abbondante quantità di fibroina necessaria per fabbricare gli idrogel, questa fase è stata ripetuta otto volte, ma solo due delle otto volte il risultato finale è stato adeguato. I principali difetti si sono concretizzati nella solidificazione della soluzione, una volta che il LiBr rimosso non poteva più evitare che le proteine si riaggregassero. Una strategia per ovviare a questo problema è di diminuire leggermente il tempo di dialisi, monitorando costantemente la consistenza della fibroina in soluzione, ed interromperla nel caso in cui questa cominciasse ad addensarsi, ma non di più di un giorno: una diminuzione eccessiva renderà insufficiente il tempo per rimuovere tutto il LiBr presente.
Un altro aspetto da non sottovalutare è la velocità con cui la fibroina, ormai isolata e disciolta in soluzione pura, possa riaggregarsi e gelificare prima dell'aggiunta degli enzimi adatti. Le cause possono essere molteplici, come gli urti tra le particelle provocati in sede di centrifugazione e scuotendo inavvertitamente la fiala contenente la soluzione nel maneggiarla. Ad ogni modo, il fattore tempo gioca sempre un ruolo negativo, per cui è opportuno sottoporre immediatamente la soluzione al protocollo di gelificazione, prima che questa lo faccia spontaneamente.

Una volta estratta la fibroina sono stati attuati i due protocolli per avviare la gelificazione tramite enzima, sia quello con l'HRP sia quello con la laccasi, riportati nel paragrafo 5.2. La realtà sperimentale ha mostrato che solo il secondo ha fornito dei buoni risultati.
Utilizzando il protocollo con l'HRP, infatti, la soluzione di fibroina non ha assunto una morfologia gelatinosa, rimanendo allo stato liquido all'interno dello stampo in silicone. Non è immediato concludere se sia stato colpa della qualità della fibroina precedentemente ottenuta o piuttosto della messa in atto del protocollo; ulteriori tentativi potranno fornire dei dati statistici più affidabili per ipotizzare un'efficacia migliore di un enzima rispetto all'altro; tuttavia, dato che a monte il protocollo di estrazione della fibroina ha funzionato solo due volte, non è stato possibile ripetere la prassi più di una volta per ogni enzima.

La ricerca si è conclusa con la prova di ossidazione dell'HMF ad opera dell'ossigeno atmosferico catalizzata dall'oro in forma di soluzione di nanoparticelle, seguendo il protocollo già esistente in letteratura, adattato allo scopo precipuo dell'indagine. I risultati ottenuti tramite analisi cromatografica dettagliati al paragrafo 6.3, mettono in luce che l'ossidazione, benché non con una resa unitaria, come dimostrato dalla presenza di HMF non reagito nel miscuglio di reazione, ha avuto luogo nel tempo di reazione dedicato; tuttavia, il prodotto ottenuto, mostra un comportamento all'esame cromatografico a metà strada tra il reagente HMF ed il prodotto desiderato FDCA, il che indica la possibile formazione di un sottoprodotto con uno stato di ossidazione intermedio, come il DFF o il HMFA. Solo un'analisi RMN potrebbe aiutare a discernere tra le ipotesi.

I procedimenti applicati in queste aree possono essere consultati per chi prossimamente si cimenterà in questa ricerca, allo scopo di confortarne i risultati, ma anche di continuarla; infatti, rimane da esplorare la fase finale del lavoro in cui le nanoparticelle ottenute vengono innestate nell'idrogel di seta per ottenere il catalizzatore ibrido.

Un aspetto interessante sarà quello di osservare l'interazione delle nanoparticelle e il meccanismo di gelificazione, operando un opportuno test reologico se è il caso.
Dopo avere eseguito il medesimo test sull'ossidazione dell'HMF con un protocollo adattato al nuovo catalizzatore, sarà possibile confrontare le performances dei due modelli: da un lato studiare la gamma di prodotti ottenuti tramite cromatografia su strato sottile o altre tecniche analitiche più raffinate come l'RMN o la spettroscopia IR, e dall'altro paragonare i tempi di reazione e la resa.

# VII. Appendice

Si riportano di seguito i 12 principi della chimica verde precedentemente menzionati

*i Prevenzione*

*È meglio prevenire la generazione di rifiuti piuttosto che trattarli o bonificarli una volta generati.*

*ii Economia dell'atomo*

*I metodi di sintesi dovrebbero essere progettati in modo da incorporare quanto più possibile nel prodotto finale i materiali e gli intermedi chimici utilizzati.*

*iii Sintesi chimiche più sicure*

*Ogni qualvolta sia possibile, i metodi di sintesi dovrebbero essere progettati per impiegare e produrre sostanze caratterizzate da un livello ridotto o dall'assenza di tossicità per la salute umana e per l'ambiente.*

*iv Progettazione di sostanze chimiche più sicure*

*I prodotti chimici dovrebbero essere progettati per assolvere efficacemente la funzione desiderata, riducendone nel contempo la tossicità.*

*v Solventi e ausiliari più sicuri*

*L'uso di sostanze ausiliarie (ad es. solventi, mezzi di separazione, ecc.) dovrebbe essere reso superfluo ogni volta che ciò sia possibile o altrimenti risultare innocuo.*

*vi Progettazione finalizzata all'efficienza energetica*

*Il fabbisogno energetico dei processi chimici dovrebbe essere considerato in termini di specifico impatto ambientale ed economico e ridotto al minimo. Laddove possibile, le reazioni di sintesi dovrebbero essere condotte a temperatura e pressione ambiente.*

*vii Uso di materie prime rinnovabili*

*Ogni qualvolta ciò sia tecnicamente ed economicamente fattibile, è consigliabile utilizzare materie prime rinnovabili piuttosto che non.*

*viii Riduzione dei derivati*

*La derivatizzazione non necessaria (impiego di agenti bloccanti, protezione/deprotezione, modifiche temporanee di processi chimico-fisici) deve essere, se possibile, ridotta al minimo o evitata, perché tali passaggi richiedono reagenti aggiuntivi e possono generare scarti.*

*ix Catalisi*

*I reagenti catalitici (quanto più possibile selettivi) sono da preferire ai reagenti stechiometrici.*

*x Progettazione finalizzata alla degradazione*

*I prodotti chimici dovrebbero essere progettati in modo che alla fine della loro funzione si degradino in prodotti innocui e non persistano nell'ambiente.*

*xi Analisi in tempo reale per la prevenzione dell'inquinamento*
*È necessario continuare a sviluppare metodiche analitiche che consentano il monitoraggio e il controllo in tempo reale dei processi allo scopo di identificare tempestivamente la formazione di sostanze pericolose.*

*xii Chimica intrinsecamente più sicura per la prevenzione di incidenti*
*Le sostanze e le forme in cui queste vengono impiegate in un processo chimico dovrebbero essere scelte in modo da ridurre al minimo il rischio di incidenti di natura chimica quali, per esempio, il rilascio di sostanze, le esplosioni o gli incendi*

(Anon., 2022)

# 1. State of the art

## 1.1 Hybrid catalysis

Catalysis appears among the 12 principles of green chemistry, defined as "*The design of chemical products and processes that are more environmentally benign and reduce negative impacts to human health and the environment*" (Paul Anastas, 1998)

More precisely, it is in the ninth principle that it finds its place: "*Catalytic reagents (as selective as possible) are superior to stoichiometric reagents".* Hence, it seems clear that more than for qualifying a specific branch of chemistry, the adjective 'green' is employed to promote an approach- a philosophy- that follows all chemical processes, with the aim of preserving as much as possible the environment and its resources.

The catalyst, a substance that promotes a chemical reaction by increasing its rate without undergoing itself any permanent chemical change, plays a crucial role. Commonly this function is performed either by a liquid dissolved in the solvent, e.g. an acid or basic molecule, either by a rare-earth metal that adsorbs the reagents and hosts the reaction.

In the context of this work, we dealt with a so-called "hybrid catalyst".

Intuitively, a hybrid material is the combination of different materials that exhibits improved properties with respect to the individual substances. It may consist only of inorganic components or only of organic components. Of particular interest are the materials constructed simultaneously from organic and inorganic components, between which there are regular chemical bonds. As an example, we can consider a material in which, for example, inorganic fibers or nanoparticles are distributed in a polymer or organic matrix and, on the contrary, organic particles and clusters are included in the structure of the inorganic matrix. (Kustov, 2021)
To avoid confusion*, "it is useful to remind the main differences between a hybrid material and a composite:*

- *Each component of the hybrid system itself has a highly organized structure at the molecular and nanoscale level, and the combination of components leads, in turn, to an additionally organized nanostructure constructed from two or more structures of components.*
- *The components of the hybrid system interact with each other to form a chemical structure.*
- *The properties of the hybrid system are determined by the set of properties of the components, while their additivity and synergy may result in new properties that were not observed in the original components."*

**(Kustov, 2021b**).

The application set of hybrid systems is quite vast: reducing energy consumption, increasing the efficiency of processes, and reducing the consumption of expensive components. The use of hybrid nanomaterials provides eco-friendly solutions for environmental problems (purification and remediation of water, air, and soil from harmful compounds), disposal of

waste (lignocellulosic waste biomass, plastic wastes, asphaltenes etc.), and the production of new fuels and products of fine organic synthesis (drugs, polymers), meeting the needs of future generations. **(Kustov, 2021**)c

The previously mentioned hybrid catalysis is then part of this last category of applications.
Hybrid catalysis is offer cost effective and is highly competitive catalysis. Among the various hybrid catalyst materials, metal NPs are gaining increasing attention. Integrating multiple functionalities into a single nanoparticle (NP) is an important strategy to design hybrid materials for advanced applications. (Park, 2021)

Hybrid catalysts with nanoparticles belong to the so-called 'core-shells' structures, the most typical example of hybrid nanomaterial: the core being the inorganic particle (metal, oxide, etc.) and the shell being formed by another material, frequently a polymer matrix.
The role of the matrix is to encapsulate the NPs and preventing their coalescence and to favor transport phenomena inside it, once that the catalytic reaction has occurred.
Also the size and shape of nanoparticles- that can vary from spherical particles, disks, tubes, or filaments to more complex shapes (stars, nested cylinders or cones, etc.)- and the interaction with the matrix have a crucial impact on the performance of the catalyst, i.e., its activity, selectivity, and stability. **(Kustov, 2021**)d

## 1.2 Furanic derivatives

The objective of the following stage is to exploit golden nanoparticles, also known as 'golden nano raspberries', whose application in the field of medicine had already been explored by Yoan Dauphin (Dauphin, 2021), as a catalyst to be injected into a matrix of a gel of silk's proteins.
The reaction on which we have focused is the oxidation of 5-hydroxymethyl furfural (HMF). The interest of performing such reaction lays not only on having an insight into the performances of the hybrid catalyst, but also on the synthesis itself of the desired product. In fact, about 90% of synthetic organic materials used in everyday life are derived from oil. Replacement of fossil carbon with second- generation biomass (cellulose) is a key factor in boosting the sustainability of the chemical industry, as it avoids fossil-$CO_2$ emission and provides a diversity of raw materials. The challenging task is to develop new catalysts that may selectively convert cellulose-derived polyols into useful products. Particular attention has been received by 5-hydroxymethylfur- fural (5-HMF). (Francesco Nocito, 2022)

The oxidation of HMF, leads to the formation of two compounds of interest which are 2,5-diformylfuran (DFF) and furan dicarboxylic acid (FDCA). These compounds can then be used in the production of bio-based polymers.
Several methodologies based on the use of chemical or enzymatic catalysis exist to selectively obtain one of these compounds. The objective of this project will be to try to develop a new hybrid method that could synergistically use a nanoparticulate catalyst and an enzyme. This will be made possible by using a silk protein-based hydrogel that can immobilize both types of catalysts in order to avoid any possible deactivation.

# 2. Nanomaterials

## 2.1 Colloids

A nanomaterial is characterized by a size of at least one of his dimensions smaller than 100 nm.
Chemical and physical properties such as ductility, conductivity and elasticity may be affected by the reduction to this scale, turning a common metal into an interesting component to a particular purpose.
The dispersion of a nanomaterial in another phase gives a colloid. (Jimmy Law, 2022)

Beside solutions and suspensions, colloid is one of the three primary types of mixtures. A colloid is a mixture that has particles ranging between 1 and 1000 nanometers in diameter. If the dimensions are smaller than this the substance is considered a solution and if they are larger than the substance is a suspension.
In colloids particles are still able to remain evenly distributed throughout the solution and do not settle to the bottom of the container. In colloids, one substance is evenly dispersed in another. The substance being dispersed is referred to as being in the dispersed phase, while the substance in which it is dispersed is in the continuous phase.
A common method of classifying colloids is based on the phase of the dispersed substance and what phase it is dispersed in. The types of colloids include sol, emulsion, foam, and aerosol.
Sol is a colloidal suspension with solid particles in a liquid. (Petrucci, 2007)

In the following paragraphs, a dispersion of solid nanoparticles in an aqueous solution will be treated, that is a sol.

## 2.2 Golden nanoparticles

Gold (Au) is the element of the periodic table identified by the atomic number 79 and electronic structure $[Xe]\ 4f^{14}5d^{10}6s^{1}$. It is a transition metal of the 6$^{th}$ group, solid at ambient temperature and with a density of 19,3 gr/cm$^3$. (Anon., 2022)
Gold's crystal structure is close-packed, face-centered cubic, using up 74% of the space, this is one of the most efficient ways for spheres to pack together. Gold shares its face-centered cubic crystal structure with copper, nickel, platinum, and lead.
Gold is a unique substance with extraordinary properties. An element, a mineral and a metal, gold occurs in nature commonly alloyed with silver but also with palladium, mercury, and copper. Adding to its allure, gold is one of only nine elements that occur in nature in its native or uncombined form.
Since it's so soft, gold can collect and form nuggets in fluvial beds and even be absorbed by trees.
That's why golden craftworks trace back to prehistorical times, as Tutankhamen's death mask (passed out in 1323 B.C.), which contains more than 100 kg of this precious metal, can witness.
Though gold nuggets as big as several feet in diameter have been discovered, single crystals are quite rare and small. Native gold crystals usually form skeletal rounded octahedrons, cubes, and dodecahedrons. Sometimes they are elongated in specific crystallographic directions

forming herringbone or dendritic twins. Others may be flattened with octahedral, cubic, or triangular faces. (Lee, s.d.)

Golden nanoparticles are mostly used for photothermic therapies, computed tomography, development of biosensors or as catalysts. Although golden NPs have a relatively high ionization energy, implying a weak molecular attraction, yet several studies have shown that gold in the form of NPs sees his catalytic properties largely boosted. Moreover, they can count on an elevated surface over volume ratio, which turns to be very useful since it allows the use of less material for a bigger surface. Consequently, their interest is at a time economic and environmental.
The typical gold catalyzed reactions include oxidation, reduction epoxidation and hydrochlorination for environmental purposes.
Currently more and more articles concern the association NPs-enzymes to form 'nanozymes', able to imitate the properties of a given enzyme or also, by adsorbing laccase onto gold, to foster its catalytic activity. (Rei, 2021)
Regarding golden catalysts' stability, it largely depends on the size of the NP: the bigger they are, less their catalytic power is effective and the less they will be stable over time. On the other hand, it is necessary to make sur that the solutions of NP produced don't tend to aggregate over time. To this purpose, the immobilization of the NP on a support, in this case the hydrogels, is to be considered an optimal solution. (Rei, 2021)**b**

Determining whether a synergy is observable in SF hydrogels containing laccase will be the aim of the following sections.

## 2.3 Synthesis of the particles

Different pathways allow the synthesis of golden NP, and they can be roughly subdivided into 'top down' and 'bottom up' processes. The formers require the possession of massive elementary gold ($Au^0$) in its reduced form, such as golden nuggets, and consist in cutting it down into small grains with appropriate techniques. The latter instead involve a chemical reaction between a mineral of gold in its oxidized form $Au^{+1}$ or $Au^{+3}$, i.e. a halide salt, and a reducing agent to induce its precipitation. In this case, the pH, the environment, the reagents, and the heating method used play a role in determining the size of the final product, which, expressed through the particles' diameter, may vary significantly in the range 1-200 nm.

The adopted protocol is due to Romain Aufaure (Aufare, 2018)**.**

In the context of this synthesis the chloroauric acid $H[AuCl_4]$ has been used, in which gold appears in the $Au^{+3}$ oxidation state. This orange-yellow Solid, ], MW= 339,79 g/mol, is a hydrophilic (ionic) protic solute. It is soluble in water and other oxygen-containing solvents, such as alcohols, esters, ethers, and ketones.

As every crystallization reaction, golden NPs requires the formation of a crystal lattice. This is obtained by reduction the of the reagent followed by its precipitation.
Therefore, a reducing agent is needed to turn $Au^{+3}$ into $Au^0$ and then a stabilizing agent must favor the nucleation and growth of the crystals in the aqueous media. During these phases,

the choice of the molecule is crucial to control the size of the golden NP, which depends on electrostatic factors.

In the experiments presented below, 1-hydroxy-1,1-methylene bisphosphonates HMBP has been used as both ligand and reducing agent and the reaction has been conducted inside a microwave reactor in basic conditions.
The following *figure 2.1* shows the general structure of a HMBP.

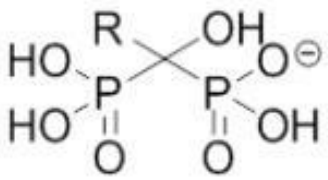


*Figure 2.1: general formula of a HMBP*

HMBP are synthetized via a multistep reaction beginning with a carboxylic acid whose alkyl chain survives intact in the final product, thus becoming the differing terminal function for each molecule of the family.

All along the experiments, we have been interested in carrying out and study two reactions in parallel, each one involving a HMBP which differed by the R- terminal:

- a phenyl (➔HMBP_Bn), MW= 303,99 g/mol
- a vinylic radical (1-hydroxy-1- phosphonopent-4-enil phosphonic acid ➔ HMBP_=), MW= 268,07 g/mol. The molecule is shown in the following *figure 2.2*

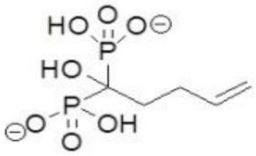


*Figure 2.2: structure of HMBP_=*

Follows the schematic representation of the reactions.

- Preparation of the golden solution:
  For this purpose, 15,52 mg of trihydrate chloroauric acid have been dissolved in 2 mL of water

- Preparation of the two HMBP solutions:
  - 12,3 mg of HMBP_= have been dissolved in 0,5 mL of water in a first moment. The pH of the solution being neuter, 340 μL of a 0,1M solution of NaOH have been added until it reached the desired value of 8,2. Finally deionized water was added up to a final volume of 1mL.
  - 57,9 mg of HMBP_Bn have been dissolved in 4,4 mL of water containing 1,64 mL of a 0,1M solution of NaOH to keep the pH close to 8,2.

- Reaction between 125 μL of the golden solution and 250 μL of HMBP_= diluted in 9,5 mL of water took place in a microwave for 30 minutes at 100°C.
  After, under the very same conditions, the same reaction was performed with the same amount of HMBP_Bn.

It is known that the properties of the NP are linked to experimental conditions, and particularly on the heating up conditions. The use of the microwave technology presents some considerable advantages in the field of chemical synthesis, especially to the meso and nano scale.
Classing heating technologies involve heat transfer via convection and conduction, that provoke an uneven volumetric repartition of the energy. The absorption of the microwaves by the liquid phase is a homogeneous process that involve two aspects: dipolar polarization and ionic conduction. The former is the rotation of polar molecules around themselves in to get aligned to the alternative electric field of the device. The latter produces the oscillation of the ions interacting with the waves and produces collisions between molecules.
These two phenomena induce a loss of energy into heat, whose amount depends on the dielectric constant of the solvent. Since the dielectric constant of water is generally greater than other non-polar organic solvents, synthesis in aqueous phase is well adapted to this type of heating (**Aufare, 2018)b**.

# 3. Characterization of the nanoparticles

## 3.1 TEM

As the pictures show clearly, the two products obtained with the different ligands have very different aspect in terms of color: the first has a vivid red color, instead the second one presents a dark brown/violet coloration.

Two different analyses have been carried out to characterize the shape and the size of the NP: TEM and DLS.

Transmission electron microscopy is one of the techniques used to characterize the obtained solution of golden NP.

The department where the experiments were conducted in UTC, TIMR, is equipped with a transmission electron microscope that allowed the analysis of the two samples of solutions obtained.

The transmission electron microscope (TEM) is a very powerful tool for material science. The TEM operates on many of the same optical principles as the light microscope but uses electrons instead of light. Because the wavelength of electrons is much smaller than that of light, the optimal resolution attainable for TEM images is many orders of magnitude better than that from a light microscope. The image is projected onto a fluorescent screen or captured by a camera if the microscope has one.
From the top down, the TEM consists of an emission source or cathode, which may be a tungsten filament or needle, or a lanthanum hexaboride ($LaB_6$) single crystal source. The gun is connected to a high voltage source (typically 100–300 kV) and, given sufficient current, the gun will begin to emit electrons either by thermionic or field electron emission.
A high energy beam of electrons passes through a complex system of electromagnetic lenses situated in the electrooptical column, and it is shone through a very thin sample, with a thickness between 50 and 500 nm. The sample is held on a tiny disk in cupper or nickel (few mm diameter) with the pattern of a net, so that the section can be observed through its holes without the interposition of a glass (differently from what happens in an optic microscope) that would be impermeable to the electrons. The latter can't pass through thick objects.
Since electrons are very small and easily deflected by hydrocarbons or gas molecules, it is necessary to use the electron beam in a vacuum environment, typically of the order of $10^{-4}$ Pa. The need for this is twofold: the allowance for the voltage difference between the cathode and the ground without generate an electric arc as well. A series of pumps are used to accomplish an adequate vacuum for this purpose.
The power of resolution (i.e. the minimum distance between two points that allows to distinguish them without collapsing the two into just one) is about 0,2 nm, that is 500.000 times bigger than the human eye and 5 times bigger than the scansion electronic microscope (SEM).
The interactions between the electrons and the atoms can be used to observe features such as the crystal structure and features in the structure like dislocations and grain boundaries. Thus, TEMs can reveal the finest details of internal structure of organelles, viruses and macromolecules - in some cases as small as individual atoms. Chemical analysis can also be

performed. TEM can be used to study the growth of layers, their composition and defects in semiconductors. High resolution can be used to analyze the quality, shape, size and density of quantum wells, wires and dots.
The light microscope and TEM are commonly used in conjunction with each other to complement a research project. (Carter, 1996), (Hirsch, 1965), (Anon., 2022)

The schema of a TEM is showed in *figure 3.1*, drawn from technology networks. (Anon., 2022)

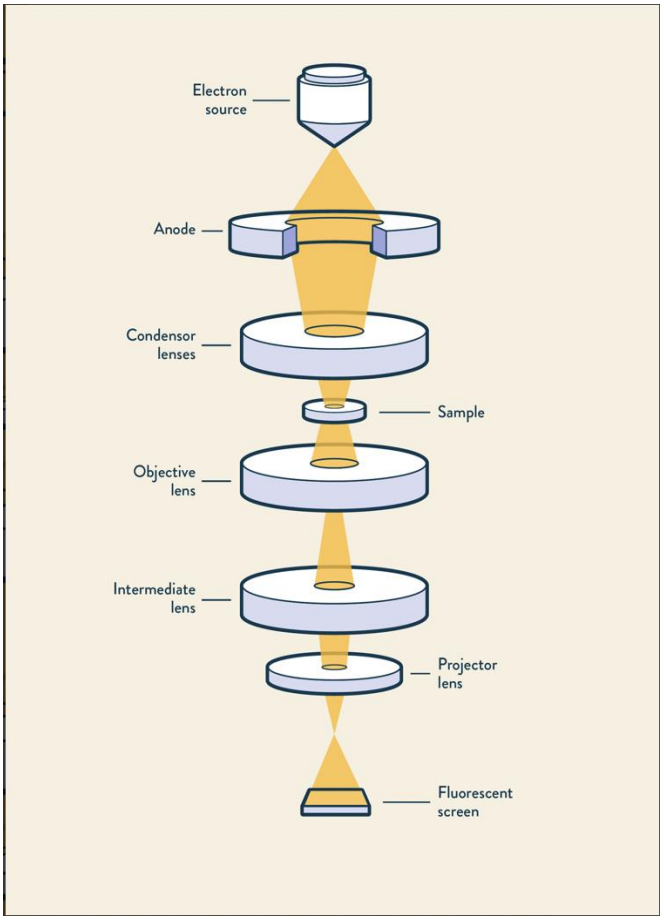


*Figure 3.1: schema of a TEM*

## 3.2 ImageJ

*"ImageJ is a software for analyzing images developed by Wayne Rasband, of the National institutes of Health."* (Sophie Allart, s.d.)
Among its main functions, one has been extremely useful to our scope: quantifying and measuring a geometrical variable along an axis in a picture. The adopted procedure consisted merely in tracing lines roughly corresponding to the diameter of the particles (whose shape is assumed to be perfectly round for the sake of simplicity). Then the length of each line was recorded in a table and compared to the reference of known length reported on the bottom left corner of the picture. Finally, these data allowed, exported into excel, allowed the extrapolation of a distribution graph, as showed in picture 4.

A series of images has been collected via TEM and reported in the following pictures.
Some are representative of the first sample, called “RED SOLUTION” the one with a red color and the others of the other one, characterized by a violet coloration.

- **RED SOLUTION**

The following *image 3.2* shows a cluster of NP in the solution.

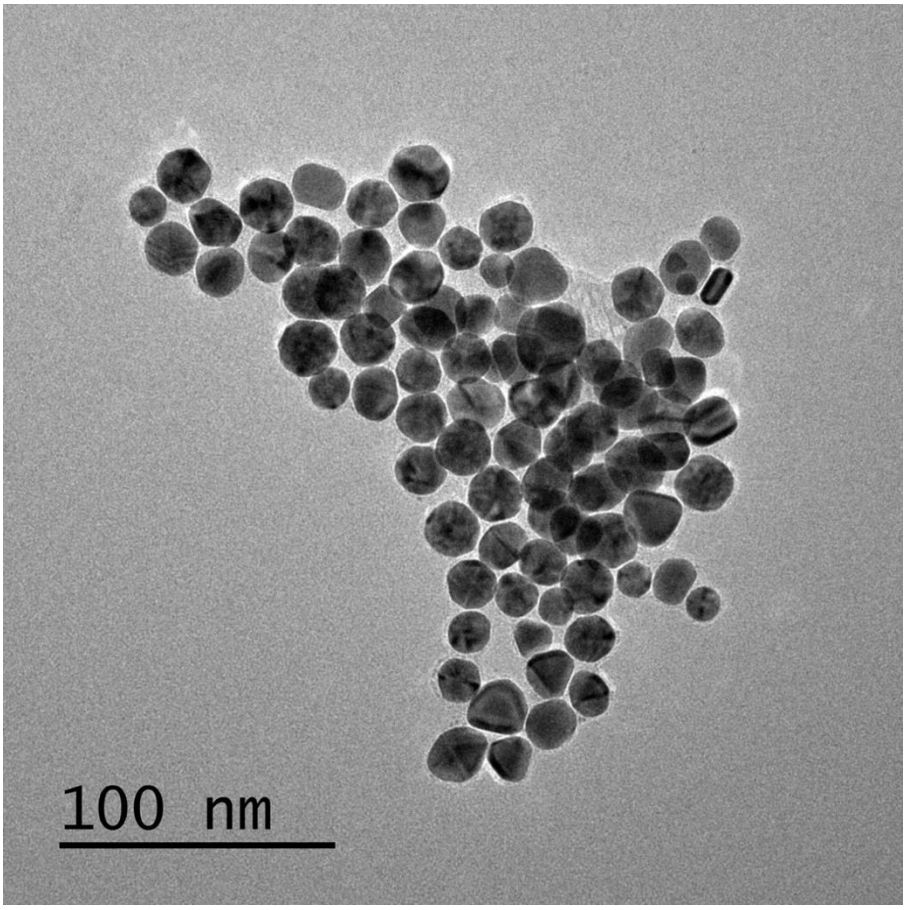


*Image 3.2 cluster of golden NP visible via TEM*

Just to have a deeper idea of the size of the NP inside other samples issued from the same solution, the following *images 3.3* show the results obtained via TEM:

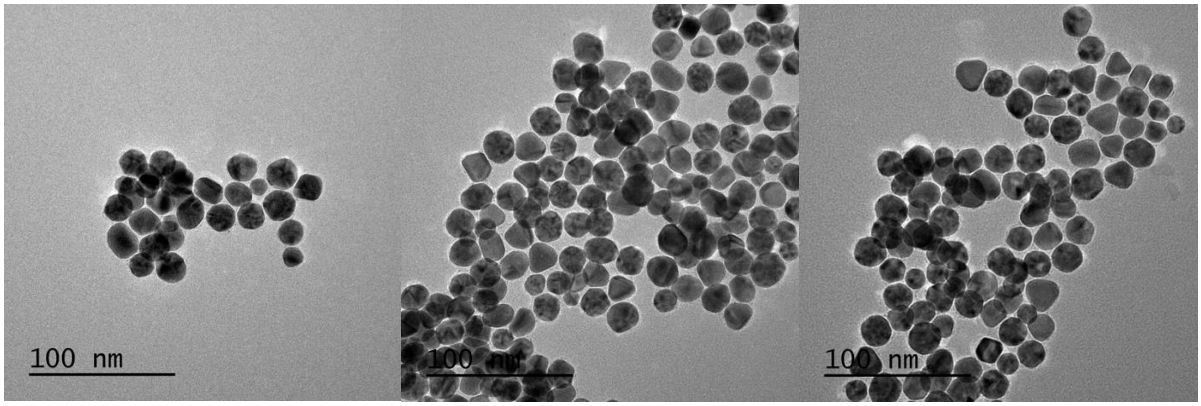


*Image 3.3 Other clusters obtained via TEM*

The following *graph 3.4* illustrates the distribution of the particles of the *image 3.2* with respect to their size.
The assumption previously made regarding their spherical size can be confirmed by the satisfying coefficient of roundness greater than 0.63 (in the range 0-1).

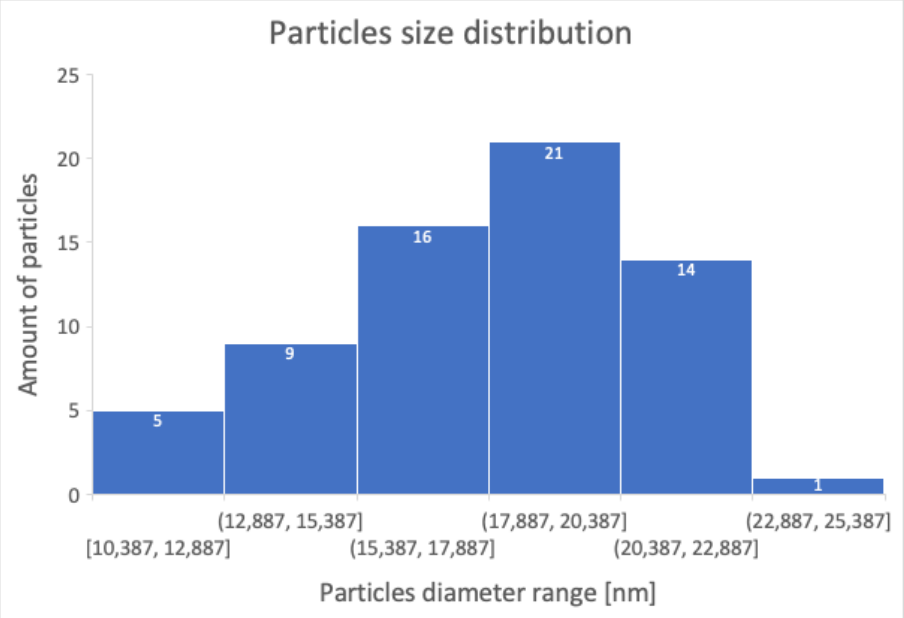


*Graph 3.4 Histogram of the numerical size distribution obtained via excel*

It appears that the average diameter is 17,83 nm.

- **VIOLET SOLUTION**

The following *image 3.5* shows a cluster of NP in this solution.

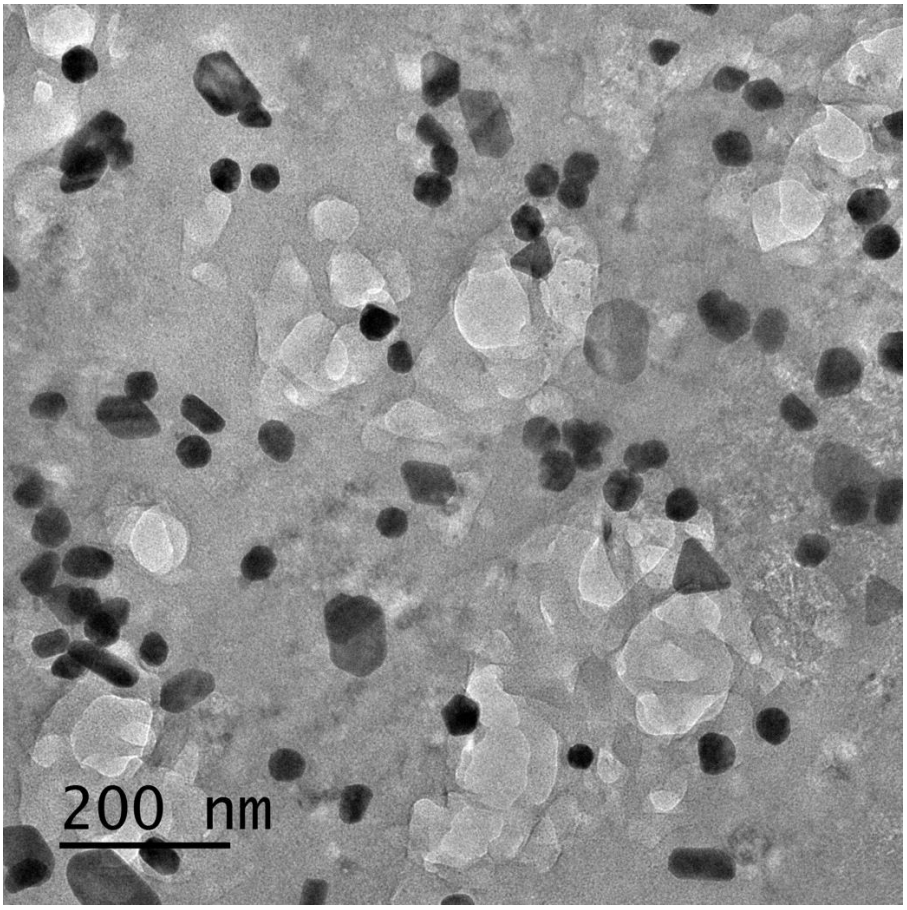


*Image 3.5: golden NP of the violet suspension observed via TEM*

Again, some other pictures of the aggregates of NP issued from the same sample:

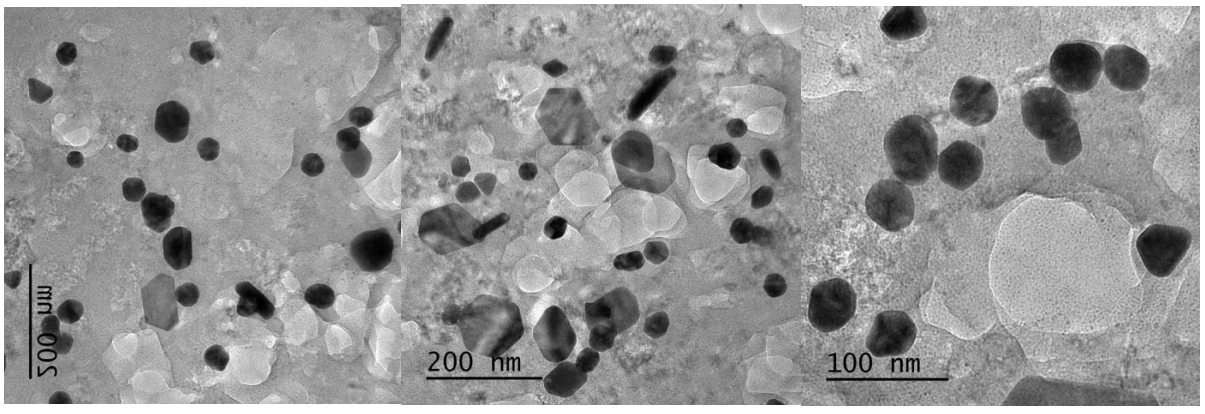


*Image 3.6: other NP of the violet sample observable via TEM*

The following *graph 3.7* illustrates the distribution of the particles of picture 4 with respect to their size.

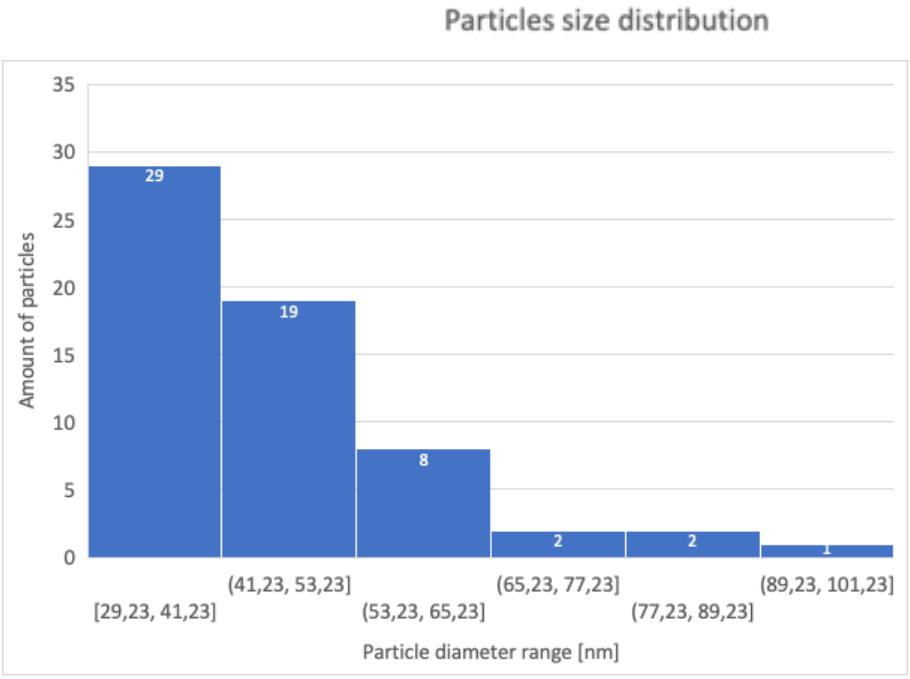


*Graph 3.7 Histogram of the numerical size distribution obtained via excel*

This time it appears that the average size is equal to 43,44 nm, i.e. more than two times bigger than the particles in the red solution.
This difference may take into account the darker shade of red of the solution, and, being the reaction condition exactly the same, must depend on the choice of the ligand used: HMBP_= instead of the HMBP_Bn.
As previously mentioned, the smaller the size the better the efficiency of the catalyst, so it is possible to forecast a more effective performance of the red solution!

## 3.3 DLS

Dynamic light scattering (DLS) is a well-established non-invasive technique also called PCS (Photon Correlation Spectroscopy) or QELS (Quasi-Elastic Light Scattering) for measuring the size of typically sub-micron molecules, nanoparticles or colloids.
In DLS measurements, the sample is illuminated by a laser beam, and the intensity changes of the scattered light are measured as a function of time. The intensity changes measured by the detector are generated by Brownian motion of the particles at the origin of the scattering. For the same temperature and viscosity, 'small' particles move rapidly - creating rapid changes in scattering intensity - while 'large' particles move more slowly - creating slow intensity changes.

Using a self-correlator, the speed of the intensity changes is measured, and the particle scattering coefficient calculated from the correlation function. (Cerini, s.d.) (Anon., s.d.)

The Stokes Einstein equation then allows the diffusion coefficient to be converted to hydrodynamic diameter.
Stokes' resistance law gives the resistance force F experienced by a particle of radius r displacement velocity U in a fluid dynamic viscosity μ:

$$F = 6\pi\mu r U$$

In addition, the diffusion coefficient is given by the laws of Brownian motion:

$$\mathcal{D} = \eta k T$$

where T is the temperature, k the Boltzmann constant and η the mobility given by the expression:

$$\eta = \frac{U}{F}$$

Using the expression for the drag force, we find the Stokes-Einstein:

$$\mathcal{D} = \frac{kT}{6\pi\mu r}$$

This law is valid for solute macromolecules of sufficient radius for the application of Stokes' law. It is modified empirically to better represent experimental results for smaller molecules. (Anon., 2022)

In the *graph 3.9* showed below it is illustrated the size distribution by number of the red solution obtained via DLS.
The statistic table provided by the software used to read the results of the analysis informs us that the average hydrodynamic diameter is 36,92 nm.
This data slightly differs from the previous result (17,83 nm); this difference must be interpretated by considering two factors:

1) The diameter here measured is not the actual diameter, but the hydrodynamic diameter.

The hydrodynamic diameter ($D_h$) of a molecule is defined as the diameter of a perfect solid sphere that would exhibit the same hydrodynamic friction as the molecule of interest. Thus, the $D_h$ value reflects primarily the hydrodynamic friction but is usually also a good estimation of the absolute size of the molecule. Generally, the more globular the shape of a molecule is, the better the $D_h$ value reflects the actual diameter.

2) The analysis via DLS has been effectuated some weeks after the TEM. Consequently, the formation of aggregation of particles moving as a whole could have taken place in the meanwhile, thus resulting in an apparently increased average diameter.

With the purpose to reduce at the least this effect, the sample of solution subdued to DLS was priorly treated with ultrasound waves, as shown in the *photo 3.8*.

*Photo 3.8: Ultrasonic tub containing the sample with the solution of NP*

The photo shows a simple device consisting of a bath where the sample is immerged. When the microwave generator is activated, the waves diffuse across the aqueous medium and enter inside the flask with the solution. Treating the sample for few seconds with this technology is supposed to reduce to the minimum the size of agglomerations of particles by dragging them apart. The physical principle of this technology is described by Priyadarshi and others:

*"Results of the ultrasonic de-agglomeration mechanism showed that ultrasound-induced microbubble clusters pulsating chaotically, were predominantly responsible for the breakage and dispersion of agglomerates. Such oscillating cavitation clusters were seen to capture the floating agglomerates resulting in their immediate disintegration. De-agglomeration occurred from both the surface and within the bulk of the aggregate. Microbubble clusters oscillating with associated emission frequencies at the subharmonic, 1st harmonic and low order ultra-harmonics of the driving frequency were deemed responsible for the breakage of the agglomerates."*
(Priyadarshi, 2021)

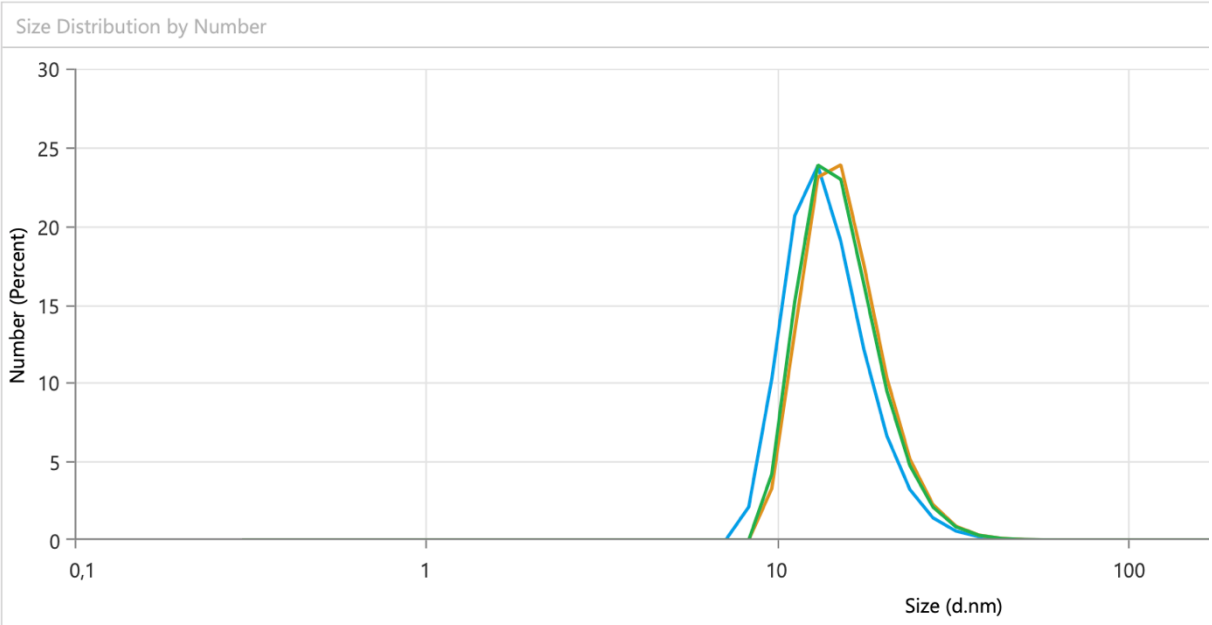


*Graph 3.9: particles size distribution by number obtained via DLS software*

# 4. Silk

## 4.1 Properties

Silk is called the "queen of natural fibers" because of its unique qualities, such as extra fineness, luster, and feel**.** (Basu, 2015)

Silk can be obtained from the cocoons of several caterpillars or silkworms.

Its fibers, despite their low elasticity, are one of the strongest natural fabrics, being stiffer than wool, also made of aminoacidic chains; their tensile strength is 740 MPa. (Rei, 2021)**b**

This remarkable characteristic can be accounted for by the molecular structure.
Silk's filaments are mainly constituted of two proteins: fibroin and sericin.
The former, which is a hydrophobic copolymer, is situated in the core of the wire, and it is surrounded by a layer of sericin, that is hydrophilic and confers to the fiber a sticky texture.
SF is largely constituted of three amino acids- Glycine (45%), Alanine (29%) and Serine (12%)- and small portions of Tryptophan, Valine and Tyrosine.
In its primary structure, these are arranged in two types of chains, a heavier chain (H-chain, ∼390 kDa) and a light (L- chain, ∼26 kDa) chain, which are covalently bound by a disulfide bond between two cysteines.
Concerning the secondary structure, three different polymorphs exist: silk I and III have coil and helicoidal structure respectively, and silk II of crystallin structure in anti-parallel β-sheets, that appears the most. Silk I corresponds to silk stored in the glands of silkworms while silk polymorph II results from exposure of the silk to mechanical and physical stress as well as exposure to methanol or water incubation procedures. These crystalline regions are primarily composed of amino acid repeats known as glycine-X where X can be alanine, serine, threonine or valine. In these regions, fibroin is thus a block copolymer made up of blocks of hydrophobic beta-sheets linked by hydrophilic separators. The result is a hydrophobic protein that self-assembles to form very strong and flexible materials. The predominance of crystalline regions in fibroin gives the materials made of it high mechanical strength and toughness. (Cristina Belda Marín, 2021)

These crystalline regions are responsible for the mechanical properties and degradation rates of silk materials. The small size of glycine allows the rapprochement of the chains, thus boosting the strength weak chemical bonds, making the wire more resistant to breakage. What is more, being a biopolymer, it is also characterized by an elevated degree of biocompatibility and degradability. Such properties are particularly appreciated and hence the numerous applications into biomedical fields. (Lancashire, 2011)

Among these, it has been found of particular interest the formation of a hydrogel hosting nanosized objects in order to provide it with tailored functions. In particular, when metal particles are obtained in an aqueous medium through a biocompatible ligand, the latter has a remarkable role to form a dispersion in SF gel that, according to Cristina Belda Marín keeps unvaried some mechanism as gelation and elastic behavior but provide it with important biological and chemical properties.

## 4.2 Silk fibroin extraction

The aim of the experience is the creation of a fibroin hydrogel for the nanoparticles previously synthetized to be injected in.

Raw silk has a natural gum called sericin. Since the formation of the hydrogel requires the extraction of SF, the very first step to operate is the removal of SS, which represents the 30% of the weight of the silk. Either way, the chemical principle of separation consists in exploiting the difference in solubility in water of the two polymers: only SS being soluble, it must be moved to the aqueous phase, so that SF can be easily recovered in the unsolved form. To do so, several methods can be used.

*"Depending on the variety of raw silk (race of silkworm), the sericin content varies from 19% to 28%. The bi-voltine silk will generally have lesser sericin content in comparison of multi-voltine raw silk. Degumming loss is the estimation of sericin that is present in the raw silk. In the silk processing units, the sericin is not fully removed; 2–3% of it is retained in silk so that, further processing of dyeing and finishing will be convenient. Total removal of sericin will lead to a deterioration of fibroin by the chemicals used for dyeing and finishing.*
*The degumming loss is estimated by different methods; however, it is opined that the following method provides results that are comparable with the best practices of industry. As per the United States method, the following materials/machines are required:*

- *Boil-off kettle: A suitable receptacle for boiling off the silk.*
- *Oven: Conditioning oven with forced ventilation efficient to dry the skeins within the time specified, positive value control, and capable of drying the sample skeins at 140 °C. It should be equipped with a balance arranged to weigh the skeins with an accuracy of 1 cg while suspended within the drying chamber. The hold of the skeins must insure free access of the dry air to all skeins.*
- *Water: The water used for all parts of the test should be of zero hardness.*
- *Soap: The soap should be properly saponified "neutral" soap in chip*

*Ten skeins, not more than one skein from one book, are taken to represent a 5 or 10 bale lot. Approximately 10 g are removed from each skein. The silk removed from the original skeins is grouped into two parts of approximately 50 g each and marked as "part number one and part number two." The samples, that is, part one and two are dried separately in the oven at a temperature of 140 °C. These are dried until the difference between successive weights taken at interval of 5 min become negligible or constant. The first weighing is made at the conclusion of the first 15 min of drying. The second weighing, made 5 min after the first weighing, is taken as the dry weight, provided that the loss between successive weightings does not exceed 1 cg.*

*The samples are boiled for 45 min in a 1% soap solution. The weight of the soap should be 25% of the weight of the sample and the water 100 times the weight of the soap. Rinsing should take place in two baths containing water at 60 °C, the volume of which should not be less than 25 times the weight of the sample. The samples are boiled again for 30 min in 2.5 l of water of*

*water per 100 g of silk, that is, 25 times the original weight of the sample (no soap). They are rinsed again, centrifuged, and dried at room temperature. The samples are weighed using the same process as earlier.*

*The difference between the dry weight of the combined weight (Parts 1 and 2) before boiling and the dry weight of the combined weight (Parts 1 and 2) after boiling is the loss in boiling-off. The percentage of loss in boiling-off should be calculated individually per Parts 1 and 2. If the percentages of loss of the two parts differ by more than 1%, the test should be repeated. The average results of the first test and repeat test should be reported."* (Basu, 2015)**b**

This protocol is the starting point in order to obtain any of the material types listed earlier—sponges, films, fibers and gels. Our protocol is designed to produce one batch from 5 g of silk cocoons, showed in *photo 4.1*;

*Photo 4.1: Intact purchased cocoons of "Bombyx mori"*

however, if more material is required, the volumes can be scaled appropriately. Only cocoons that look undamaged should be used in the process. If necessary, silk cocoons can be replaced with bave fibers (raw silk textile yarn) and the remainder of the protocol can be used without changes.

The extraction procedure followed in the experiments is the one due to Rockwood & others**.** It consists of four consecutive steps:

1) Before the extraction it is necessary to cut 5g of cocoons of "Bombyx mori" in small fragments using a pair of scissors. After this prior step, these pieces must be transferred into a 2L beaker containing a 0.02M boiling solution of sodium carbonate $Na_2CO_3$ (i.e. 4,24g) and provided with a magnetic stirring bar (see *photo 4.2)*. To prevent boiling over the carbonate must be added slowly. This salt provokes an alkaline hydrolysis, thus withdrawing the external layer of SS. If this step is repeated several times with different cocoons, each time must last the same so that the average MW of the SF is identical. Moreover, heating too much could spoil SF. The chosen duration is 40 min. For samples that have been degummed for 30 min, the molecular weight has a broad distribution centered near 100 kDa. This value can increase for

shorter degumming times or decrease when degummed for longer times. Occasionally it is useful to stir the skeins with a spatula to promote dispersion.

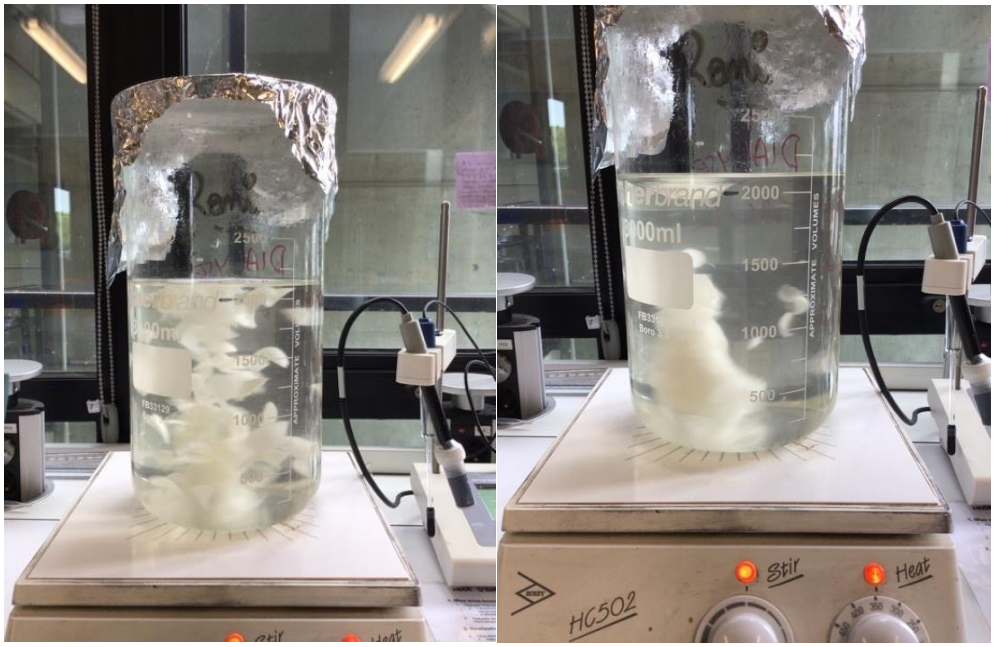


*Photo 4.2: Beaker containing the integer cocoons in the degumming solution, after 5 min (left) and 25 min (right)*

Afterwards the obtained fibers, who are supposed to look like a flock of hydrophile cotton (reference in *photo 4.3*), are to be rinsed with pure water in order to wash off the residues of carbonate and SS; it is recommended to repeat this passage at least three times. Finally, after discarding the liquid and squeezing the flocks with hands, the SF must be placed on an aluminum foil under a fume hood to let water evaporate for 12 hours. Degummed silk fibroin, in which the sericin has been removed, can be stored indefinitely at room temperature.

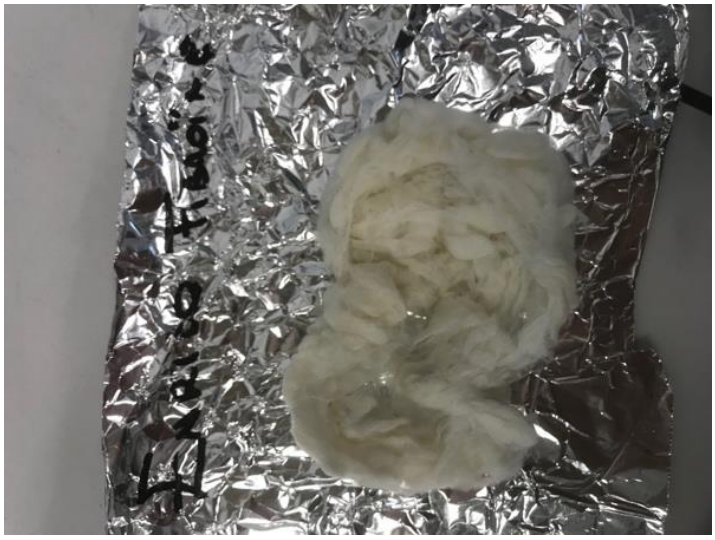

*Photo 4.3: skein of pure fibroin*

2) The second step is a dissolution step of fibroin fibers in an aqueous solution of 9.3M Lithium Bromide (LiBr) at 60°C (inside an oven) in order to proceed to a denaturation of fibroin proteins. We decide to opt for the same dissolution time of 4h for each synthesis.

   To do so, the SF obtained has been dry weighted, then it was covered with a solution of LiBr. Knowing that the MW of LiBr is 86,85 g/mol and that the volume requested to properly wet the SF is given empirically by:

$$V_{LiBr} = 4 * m(SF) * \frac{mL}{g} + 5mL$$

   The amount of LiBr to be dissolved is easily calculated by:

$$m_{LiBr}[g] = V_{LiBr}[mL] * 86{,}85\frac{g}{mol} * 9{,}3\frac{mol}{L} * \frac{1L}{1000mL}$$

   Once the silk fibroin is completely dissolved, it will appear amber in color and will be transparent, as *photo 4.4* certifies. Black bits from the silkworm may be visible but will be removed later. This solution will be highly viscous but should not contain any intact fibers, as determined by visual assessment.

*Photo 4.4: fibers of silk fibroin immersed in the bath of LiBr solution after 4h incubation*

3) The third step consists in dialyzing the obtained solution with water to remove as much Lithium Bromide as possible from the SF. The viscous solution must be injected with the help of a 18-gauge needle and a 20 mL syringe inside 3.500 MWCO 'Thermo Fischer Scientific' cassettes for dialysis as the one in *photo 4.5*. Be careful not to puncture or touch the dialysis membrane. The solution will be very viscous, and this step will be easier if the solution is kept warm before adding to the cassette. It is important to avoid shearing the solution whenever possible to avoid the induction of β-sheet within the silk. Therefore, only use the needle when injecting into the cassette.

Moreover, have an additional needle and insert it into another top port of the cassette to allow air to escape. Remove the extra needle once all the air has been purged.

The cassettes must be wet in water for 3 minutes in advance. A total of 6 water changes of 2L volume will be performed over a 72h period but at different intervals (more frequent changes during the first hours).

*Photo 4.5: dialysis cassette filled with SF solution*

4) The fourth and last step is the centrifugation of the dispersion. After collecting the SF from the cassettes with the help of the syringes, centrifugation is carried out twice for 20 minutes at 3°C and at 9,000 rpm and allows to remove the insoluble impurities from the SF.

(Danielle Rockwood, 2011)

This SF supposed to look like *photo 4.6* can then be stored in the refrigerator (4°C) for about 1 month because beyond this time the solution gels. It is also necessary to pay attention to the mechanical constraints, as well as to the variations of pH and concentration that SF can undergo. Indeed, these could cause a rearrangement of the proteins in the form of beta-sheets and thus gel the solution. (Cristina Belda Marín, 2021)**b**


*Photo 4.6 SF recovered at the end of the extraction*

Once that SF is recovered, the mass concentration of SF must be preliminarily calculated. The method used is the dry weigh method:

1) An empty boat is weighted ➔ $M_1$
2) 500 µL of the solution of SF is added and then it is weighted again ➔ $M_2$
3) The boat is left overnight inside an oven at 60°C to evaporate water, then the dry residual is weighted ➔ $M_3$
4) The following relations give the concentration expressed in different ways:

$$C^{SF}_{\frac{w}{w}\%} = \frac{M_3 - M_1}{M_2 - M_1} * 100\%$$

$$C^{SF}_{\frac{w}{v}\%} = \frac{M_3 - M_1[g]}{0{,}5\ [mL]} * 100\%$$

The overall yield of this preparation can be estimated with the help of the following expression: $r_{SF} = \frac{m_{SF}}{m_{cocoons}} * 100\%$

## 4.3 Troubleshoots

Since the protocol of extraction of the SF has been repeated several times throughout the experience, it was possible to notice all his downsides and troubleshoots, and consequently to point out some critical steps which require a deeper attention from the chemist.
In the following lines some of them are illustrated with the attempt to ameliorate this technique.
The same numeration is used to refer to the steps of the precedent paragraph:

1) Two aspects deserve a particular attention:
   - The choice of the cocoons to cut, avoiding the ones with a yellow coloration, which may contain traces of the shell of the silkworm, that will pollute the SF until the centrifugation and are really annoying to remove
   - Envisaging an adequate time of evaporation under the fume hood; The swab of SF has an elevate capacity of absorbing water, as the weights recorded before and after evaporation can prove:
     - Mass of the cocoons ($M_1$) = 5g
     - Mass of humid SF after extraction ($M_2$) = 12 g
     - Mass of dried SF after 24hr = 3,47 g (this confirms the estimation of the composition of silk 70% w/w fibroin)

2) The dissolution of LiBr in water is extremely exothermal and may lead to the formation of crystals. To prevent this hazard, it is recommended to add little by little the salt into a vigorously stirred beaker. LiBr has a low density, and its volume should be taken into account while preparing the solution. We suggest adding only 60% of the calculated volume of water and then bringing the solution up to the final volume. The best technique to correctly wet the fibers is to pour the solution on them and not to incorporate the fibers in the volume (in fact it would be an approximately 20%$_{w/v}$ mixture and SF fibers are very light and fluffy).

3) When the solution that underwent dialysis is extracted from the cassettes, it is of the utmost importance to reduce to the minimum the mechanical constraints. Also passing through a tight needle, flowing inside a syringe, being shaken inside a tube are events that may induce the reaggregation and gelation of the proteins. In fact, during dialysis LiBr is removed, and with it its denaturation power, so step 2) may be reversed. Two alternatives are possible: either the dialysis cassettes are to be replaced by a simple membrane bag with the pores of the same size, either the membrane of the cassettes must be cut with the tip of a knife, thus letting the SF exit without being once more aspired by the syringe.

Knowledge of the interactions between peptide groups and water or denaturing agents is of major importance in understanding proteins. the increased viscosity of proteins in strong lithium bromide solutions is the result of more extensive bonding and more helical coiling than in water, in lithium bromide solutions there may be lithium to carbonyl bonding or bonding of carbonyl to water of the lithium hydration sphere. The multiplicity of hydrogens in the hydration sphere of lithium would permit formation of larger aggregates than in water. At low peptide concentrations, multiple binding becomes less probable, and there may be only one peptide group bound for each lithium. The nature of the lithium to peptide bonding is not specified but may be similar to the ion-dipole attraction of lithium to water. The increased viscosity of proteins in strong lithium bromide solution may be due to extension of the polypeptide chain as a result of attaching many hydrated lithium ions in close proximity. (J. Bello, 1961)

Always concerning this passage, it is worth to describe a phenomenon that occurred when another kind of degumming process was used instead of the one of step 1) and whose results appeared during the second and third day of dialysis. In this case, the cocoons were not degummed at 100 °C and pressure atmosphere inside a 2L beaker covered with an aluminum foil as usual, but a higher-pressure method was used. As a matter of fact, a batch pressured tank with 1,5 atm of relative pressure would increase the boiling temperature of water, thus making the degumming faster and more effective. Nonetheless, this technical choice is opted when the interest of the degumming is just to recover SS, because the effects on the structure of the SF have proven to be irreversibly destructive. As visible in the photo 4.7 below, the viscous solution of SF tended to solidify, assuming a wax-like texture. The block was rigid but light, crushable barehand. For the sake of deeper investigation, the concentration of SF in the brine that accompanied the product inside the cassette was strongly reduced due to the agglomeration in the solid phase. The origin of this stabilization is presumed to be linked with the cutting down of the polypeptide chain of SF caused by the more aggressive conditions of degumming. Smaller fragments of the protein have higher mobility in the liquid phase and, fostered by diffusion and the mechanical constraints originated from the stirring, can form bindings and collapse. A result is shown in *photo 4.7*.

*Photo 4.7: Accidental coagulation of SF occurred during a failed attempt of extraction*

# 5. Hydrogels

## 5.1 Interest of the hydrogels

Hydrogels are three-dimensional network structures able to imbibe large amounts of water. Hydrogels do not typically dissolve due to chemical or physical cross-links and/or chain entanglements. They exist naturally in the form of polymer networks such as collagen or gelatin, or can be made synthetically.

The capacity of hydrogels to absorb and retain a large volume of liquid makes them interesting for depollution purposes, particularly in the context of the elimination of hazardous substances present in the environment. Environmentally sensitive hydrogels can serve a wide variety of applications because of their ability to respond to environmental changes, typically by exhibiting changes in volume. Traditional stimuli that elicit hydrogel response are pH, temperature, and ionic strength. Analytes and biomarkers including glucose, proteins, and DNA also elicit hydrogel responses. Because of such a wide variety of response triggers, hydrogels can be incorporated into sensors or actuators, or can be utilized in controlled drug delivery systems, biosensors, tissue engineering scaffolds, artificial organs, wound healing bandages, physiological membranes, contact lenses, and microfluidic valves. (N.A. Peppas, 2012)**,** (Rei, 2021)**c**

Gelation is an important process for a wide range of applications in food, pharmaceutical, and material sciences. A common feature to all protein gelation reactions is that they require some initial structural transition that can be considered transformation from an unreactive to a reactive structure that increases the probability of intermolecular interactions. (Erik van der Linden, 2009)

Gelation has been described as the association or cross-linking of long polymer chains to form a three-dimensional continuous network which traps and immobilizes the liquid within it to form a larger crystal structure than initially that is resistant to flow, under pressure.
The main constituents responsible for gelation are colloids of carbohydrates and proteins. Thus, the more the hydrogel is concentrated in protein, the more the hydrogels formed are resistant to compression and deformation. This is due to a more compact molecular network that allows for better stress distribution.

The mechanisms of gelation remain poorly understood. The mechanism involved in gel formation for proteins are complex and may involve salt bonds between amino and carboxyl groups in the side chain, hydrogen bonding between peptides and disulphide cross-linkage. Instead, most carbohydrates require heat for gelation (e.g., pectin); this is believed to provide energy to alter the structure of the molecule, making it more amenable to cross-linking. Often specific ions are required to complete the gelling process; furthermore, the gel network may then shrink during storage, liberating free water, this process being known as weeping or syneresis.
Factors involved in gelation are the formation of random chains and cross-linking of the chains, either by hydrogen bonds or by salt bridges. Some gels are clear and thermally reversible, e.g. gelatin; others are cloudy or opaque, e.g. egg white.

The gelling ability of most proteins is affected by the pH, temperature, degree of swelling, the ionic environment and the presence of other substances.
Gelation can be measured in two ways. The first involves measuring the time for a solution of the material to form a gel when it is heated at a constant temperature. For proteins, the concentration used is between 8% and 12% and temperatures between 80 °C and 140 °C.
The second method involves measuring some rheological property of the gel such as strength, hardness or compressibility. (Lewis, 1996)

## 5.2 Chemical gelation

The protocols presented in the literature to control the formation and characteristics of hydrogels describe two main techniques: physical and chemical gelation. Physical gelation can be induced by applying a physical force and relies on the formation of non-covalent bonds between SF chains. However, it will not be treated in this study because we focus on chemical gelation. This is caused by the formation of covalent bonds in the presence of an enzyme, a chemical catalyst or another chemical species.
We are particularly interested in enzyme-assisted cross-linking because of its low toxicity. In addition, the catalyzed enzymatic reactions are very specific and allow a good control of the obtained product.

On the other hand, immobilization of enzymes on a support, such as a hydrogel, allows for greater stability of the enzyme. This preserves its activity and functional structure because it is physically trapped in a host matrix, in this case the fibroin polymeric network constituting the hydrogel. (Rei, 2021)**c**

In this study, the hydrogel in question is with the previously synthetized SF as well as an enzyme. Concerning the incorporation of the NP solution, at a first attempt it was chosen to replace it with water, because the goal was to test the efficacity of the gel formation and only subsequently the synthesis of the actual hybrid catalyst.
Two different pathways will be discussed in the next subparagraphs, each using a different enzyme: Laccase and HRP.
When golden NP solution is used instead of water, the two protocols that follow are to be considered basically unchanged, except for the obvious replacement of this constituent.

### o Laccase

Laccases (EC 1.10.3.2 diphenol oxygen oxidoreductase) has been known already since the 1880s when it was first described in the lacquer tree). Laccases belong to a superfamily of (multi copper oxidase) MCOs forming a phylogenetically divergent group of so-called ‘blue oxidases’, all of which contain four copper atoms per enzyme molecule, arranged into three metallocenters between three structural domains formed by a single polypeptide of about 500 amino acids in length. Laccases usually have masses of 60–80 kDa.

They are naturally produced by different plants, bacteria, insects and fungi, but they are also relatively easy to produce heterologously in industrial host organisms.

They are also rather robust enzymes and can be used in the presence of various organic solvents. Thus, they are excellent catalysts for industrial processes.

Laccase utilizes the reduction of molecular oxygen to water to oxidate substrate molecules. Since they have a low substrate specificity which means that they can oxidize a wide variety of molecules of both natural and industrial origin. The main substrates are phenols and arylamines.

In this case, we use a Laccase produced by a white rot fungus called 'Trametes versicolor'. Regarding its stability, it has been reported that Laccase is most stable at slightly acidic pH (between 3 and 5,7) and becomes less stable at lower pH. To ensure optimal operating conditions, however, the enzyme/substrate couple must also be considered, not just the enzyme. The optimal pH value for this couple can then vary.

The interest of Laccase in hydrogel formation is that it acts as a biocatalyst: it allows to catalyze modifications at the level of proteins and peptides by forming peptide-peptide or protein-protein cross-links. The oxidation of peptide or protein molecules is carried out thanks to the tyrosine residues present by forming intermolecular di-tyrosine cross-links. Thus, it could be used as a catalyst for cross-linking and thus the formation of hydrogels.
(Rei, 2021)**d**, (M. Tuomela, 2011)

### Protocol

As anticipated few paragraphs before, the propaedeutic step to synthetize the hydrogel is to evaluate the SF concentration in the solution to jellify.

The data collected with the method of the dry weights are:

$M_1$= 0,6325 g

$M_2$= 0,9107 g

$M_3$= 0,6467 g

Therefore, by applying equation N. We obtained on a weight and volume basis respectively:

$C^{SF}_{w/w}$= 5,1%

$C^{SF}_{w/v}$= 2,84%

The volume concentration of the reticulating agent, Laccase, is 2,31%. As a consequence, the volume of SF to use will be a function of the desired volume of gel and of its fibroin concentration according to the identity:

$$V_{SF} = \frac{\frac{2{,}31}{100} * V_{gel}}{C_{SF}}$$

Obviously, the volume of enzyme to incorporate depends on the amount of active Laccase that we want to use to reticulate the fibroin and form the gel. In this case study, the selected activity for the hydrogel is 1,5 U, instead the original specific activity of the used Laccase is 247 U/mL. Finally, for the sake of simplicity, it was chosen to synthetize a volume of gel equal to 1mL. The reason for this technical choice lies on the availability of the silicon mold with cylindrical holes used as a support for the hydrogels.

It is then immediate the calculation of the volume of Laccase solution to use:

$$V_{Laccase} = \frac{A_{gel}}{A_{sp}{}_{Laccase}}$$

Which gives: $V_{Laccase} = \frac{1{,}5\ U}{247\frac{U}{mL}} = 6\mu L$

The last element is the volume of water needed to reach the desired total volume of gel, set to 1mL as already stated.

$$V_{water} = V_{gel} - V_{SF} - V_{Laccase}$$

And with our data, the result is:
$V_{water} = 1mL * \left(1 - \frac{2{,}31}{5{,}1} - 0{,}006\right) = 0{,}54mL$

This volume of water is poured in a beaker of 20mL and enriched with elementary oxygen via gas bubbling; for that, a pipe of compressed air is immerged inside the beaker, perfectly still, and activated for 5 minutes. The oxygen that will dissolve in water according to the Henry's Law will provide the oxidant needed by Laccase to perform the reaction.

The procedure is extremely simple, and it just consists of mixing in a beaker with the aid of a micropipette the constituents in the following order: oxygenated water ➔ SF ➔ Laccase.

Once that the solution is prepared, it must be used to fill the holes of the mold, always using the pipette. The mold should then be placed in a glass desiccator containing two beakers full of water to create a moisty atmosphere, thus preventing an excessive evaporation of water from the jellifying solution.

The gelation time required may vary as a function of $V_{gel}$ and $V_{Laccase}$, but normally within the range 24-72 h.

When the process is over, the gels are removed from the holes of the mold with the aid of a spatula and stored at 4°C inside a flacon of pure water.

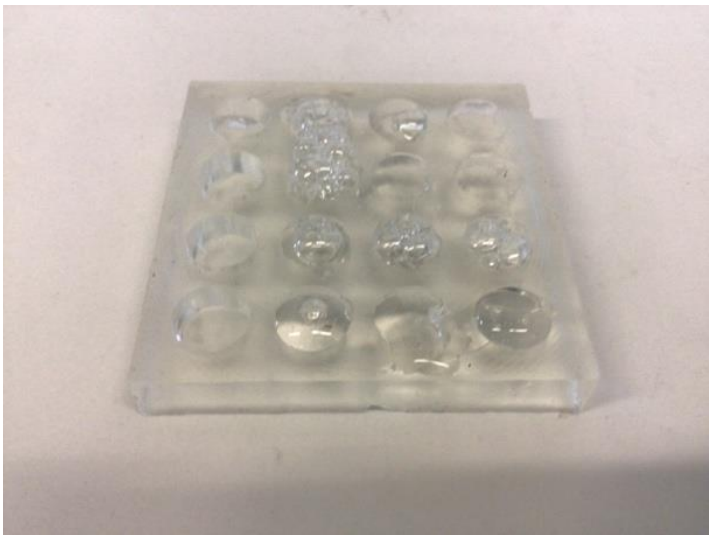

*Photo 5.1: mold with SF hydrogel*

*Photo 5.2: 4 units of SF hydrogels obtained after gelation*

- HRP

The enzyme horseradish peroxidase (HRP, EC 1.11.1.7), found in the roots of horseradish, is a metalloenzyme of molecular weight 40,000 with many isoforms, of which the most studied type is C. It catalyzes the oxidation of various organic substrates by hydrogen peroxide.

HRP is a member of the large class of peroxidases, which are enzymes defined as oxidoreductases using hydroperoxide as electron acceptor. Due to its commercial availability in high purity, HRP has long been a representative system for investigating the structure, dynamic, and thermodynamic properties of peroxidases, especially for understanding their biological behaviors of catalyzing oxidation of substrates by $H_2O_2$.

The reaction of HRP with its fundamental substrate, $H_2O_2$, forms a stable intermediate that can dissociate in the presence of a suitable electron donor, oxidizing the donor and potentially creating a color change. The donor can consist of oxidizable molecule. (Hermanson, 2013)**,** (Shengshui Hu, 2008)**,** (Anon., 2022)

Protocol

In this case, to form SF hydrogels the SF dispersion must be mixed with water in a 1:1.6 ratio. Gelation is induced by adding 10 µL of HRP (1 unit/µL) and 10 µL of $H_2O_2$ 1% .

Gelation can be carried out in PDMS molds for easy post manipulation and in a glass desiccator in the presence of two water-containing beakers to increase humidity and avoid evaporation. The gelation time is dependent on the mold volume (4−72 h). (Marin, 2021)**c**

## 5.3 Characterization of the hydrogels

After waiting the canonical 72 h to observe the gelation process, it was decided to advance in this research by observing on a microscale the phenomenon that had taken place to transform the SF solution into the hydrogels. Among all the physical-chemical analysis techniques, the one that fitted best for this purpose was scanning electron microscopy (SEM).

SEM is an analytical instrument that makes it possible to observe the morphology of materials magnified up to 100,000 times, over areas of a few mm2 and with a resolution varying from 1 to 20 nm, while also shedding light, through appropriate instrumental modifications, on other features of the substance examined such as the average and local atomic composition, differences in atomic composition between various parts of the area examined, etc.
There are many similarities between SEM and the previously discussed TEM; Also in this case, The instrument consists of a vacuum column, at one end of which is the source, an electron emitter, or 'gun' (typically a tungsten cathode, W, or lanthanum hexaboride, LaB6) that is accelerated against an anode at the other end. The electron beam is collimated by a series of magnetic (condenser) lenses that narrow its diameter down to 0.5÷5 nm (SEM's beam is more focused with respect to the broad electron beam of the TEM); these are followed by other magnetic (scanning) lenses that deflect the beam so that it intercepts the sample according to a small rectangular area and moves it both horizontally and vertically across the examined surface. Adding up the sequential recordings of these small areas on a screen or solid-state detector gives the complete image of the area. When an electron beam strikes a material, two types of radiation are generated: secondary electrons, which are emitted by the sample, and backscattered electrons, that is, the portion of incident, primary electrons that are not absorbed by the sample being sent backward. With appropriate detectors in the SEM, one or the other can be isolated: maps obtained with secondary electrons are sharp, but they reveal mainly the topography of the sample, that is, how its constituent parts are distributed in the plane; maps of backscattered electrons, on the other hand, reveal its morphology, since, although they are less sharp, they have greater depth of focus and thus highlight the highs and lows, that is, the three-dimensional shapes of the sample.

TEM and SEM differ in how they work and what types of images they are able to capture, the types of samples that they require, the resolution of images that they create, and more. Even

the basic microscope setup is different. In SEM, the sample, located at the base of the electron column, is scanned and the resulting electron scattering is analyzed to produce an image. In TEM, the sample is placed in the middle of the microscope and electrons pass through the sample before being collected. TEM offers information on ultrathin samples' inner structure, while SEM records information about a sample's surface.
Basically, SEM is faster, cost less, requires less sample preparation, but offers a 2D image, with a smaller resolution (25 times less powerful than TEM). (Anon., 2022)

The *figure 5.3* taken from technology networks beneath illustrates the structure of a SEM:

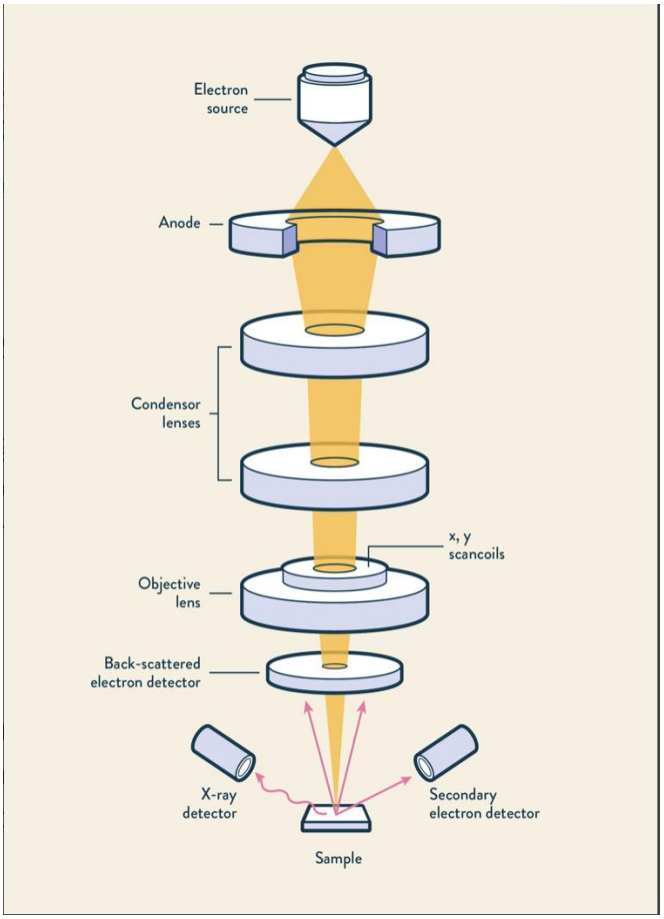


*Figure 5.3: schema of a SEM*

For being observed via SEM, the hydrogels have been priorly freeze-dried. For doing so, they have been placed in a freezer at -80°C for some hours. Then, they have been put inside a freeze drier to remove water under vacuum conditions, thus obtaining a powder solid structure that could be prepared to become the specimen of the SEM.

The *images 5.4* collected after this procedure are reported underneath:

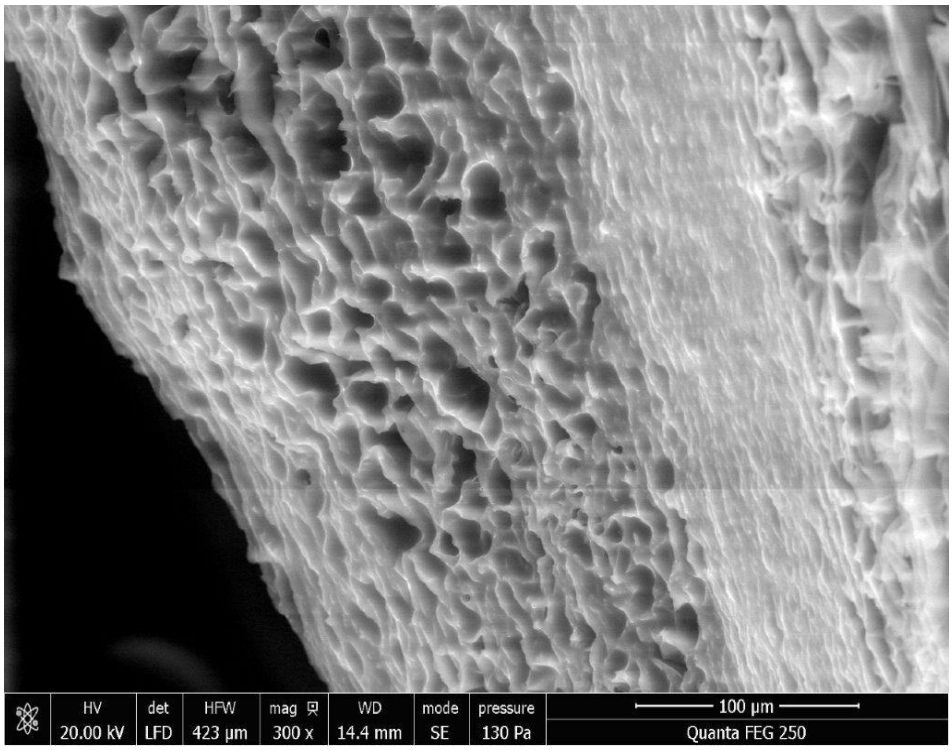


*Image 5.4: structure of SF observed via SEM*

In the image it is possible to clearly appreciate the entanglement of the fibroin in its three-dimensional structure after that gelling has taken place. Holes and pores are present in the uneven surface of the gel, becoming cavities to host air, event responsible for the swelling the gel.

# 6. Key reaction

## 6.1 HMF

The targeted reaction is the oxidation of 5-hydroxymethyl furfural (HMF), whose chemical formula is $C_6H_6O_3$, with MW= 126,11 g/mol.
*Figure 6.1*, drawn from Wikipedia, shows the 2D chemical structure of the molecule.

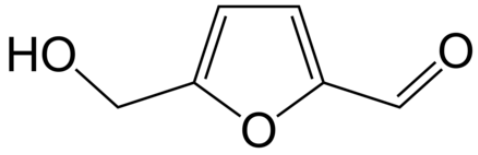


*Figure 6.1: chemical structure of HMF*

5-hydroxymethylfurfural is a member of the class of furans: it is a bi-functional heterocycle, that is furan which is substituted at positions 2 and 5 by formyl and hydroxymethyl substituents, respectively. Virtually absent from fresh foods, it is naturally generated in sugar-containing foods during storage, and especially by drying or cooking. It has a role as an indicator and a Maillard reaction product. It is a member of furans, an arenecarbaldehyde and a primary alcohol. (National center for Biology Information, 2022)
It is a white low-melting solid (although commercial samples are often yellow) which is highly soluble in both water and organic solvents.
5-HMF can be considered a prominent building block: because of the presence of the alcohol and aldehyde moieties, it can be used to generate useful molecules as chemicals of industrial interest with high added value, monomers for polymers, and even fuels. (Francesco Nocito, 2022)**b**

This organic compound produced from biomass is formed by the dehydration of reducing sugars and is a non-competitive product with the food oxidic fraction. Lignocellulosic biomass can be converted via an acid catalyzed transformation consisting of two steps, the first one is cracking the long carbon chains of lignocellulose and starch into a series of $C_5$ and $C_6$ carbohydrates, and those products can be further reformed by dehydration, to form principally platform molecules, such as furfural (FUR), and 5-hydroxymethylfurfural (HMF). (Erwann Guénin, 2022)

The *figure 6.2* underneath outlines the most important fuel and chemical products derived from HMF mainly by oxidation. (Picture taken from **Metal vs. Metal-Free Catalysts for Oxidation of 5- Hydroxymethylfurfural and Levoglucosenone to Biosourced Chemicals** with modifications)

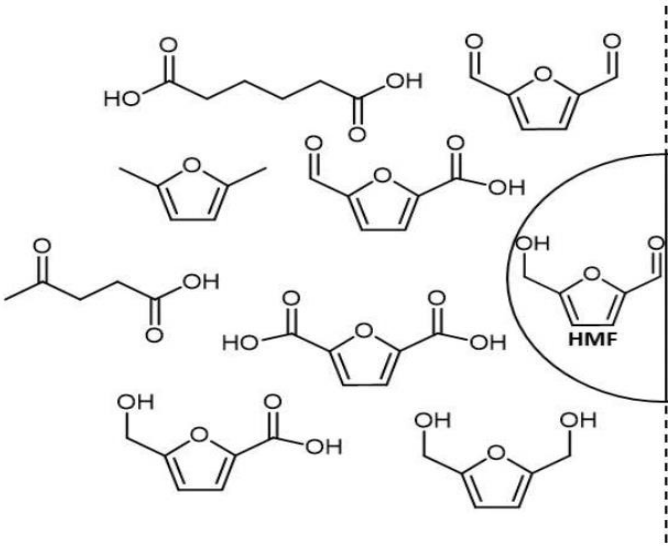


*Figure 6.2: spectrum of all the oxidated forms of HMF*

There is a giant number of ways to potentially transform these platform molecules into fuels and functional chemicals. Usually, HMF can be either reduced to a diol or oxidized to a diacids. These two compounds are used for the synthesis of polymers. In addition, hydrogenation is used to upgrade HMF into fuel molecules. The traditional valorization processes of these bio-sourced molecules used metal catalysis, usually with noble metals to obtain good conversion, yields, and selectivity. Though catalysis is one of the pillars of green chemistry, the use of expensive, toxic and critical metals is often detrimental to this appellation. Therefore recently, alternative types of catalysis have attracted the attention of scientists and researchers and such catalysts can be considered as green catalytic materials, because they can be highly efficient, easy to handle, environmentally friendly and economical in various industrial sectors. This dynamic was motivated by the desire to overcome the disadvantages of metal catalysis and by the interests that can be gained from their substitution.

Several metal heterogeneous and homogeneous catalysts, mainly based on Pt, Pd, Au, Ru, Ir, Re, Rh, V, Ni, Cu, and Co metals, have been extensively studied in various catalytic transformations to efficiently upgrade furan derivatives. Several recent reviews have dealt with the subject of oxidation by metal catalysis, and readers may refer to them. For example, there are methods of oxidizing 5-HMF for its transformation into 2,5-furandicarboxylic acid (FDCA), 2,5-diformylfuran (DFF) and maleic acid. One notable case is the base free oxidation of furfural and HMF on supported gold catalysts. With its exceptional catalytic properties and its inertia to oxidation naturally, Au has been studied in depth for oxidation transformations of furanic derivatives and especially HMF due to its application in the synthesis of FDCA. As it could be predicted, HMF is oxidized very effectively in its presence. The classic conditions are to use nanoparticles dispersed on a support, to use oxygen as an oxidant and to work in a basic medium, which greatly improves the kinetics of the transformation. The results obtained are generally very good, even excellent, however the separation of the FDCA from the reaction medium is a major problem due to neutralization and the presence of inorganic salts resulting from the bases used.
In some cases, the structure and size of the nanoparticles is critical and can strongly affect the yield, the smallest being the most active. (Erwann Guénin, 2022)**b**

## 6.2 Oxidation protocol

Guided by Professor Gérald Enderlin, the solution of golden NP was tested in an oxidation reaction of the key reactant.

Of course, this step is a preliminary to the actual hybrid-catalyzed reaction in which the oxidation is boosted by the SF hydrogel enriched with the above mentioned NP; the aim is to set the "zero" of the reaction, i.e. the second term of comparison, thanks to which we can compare the performances of the hybrid catalyzed reaction with respect to the simple gold catalyzed one to establish if a constructive synergy derives from injecting the NP inside the silk hydrogel.
This prior experiment is twofold useful because it also allows us to have an insight into the spectrum of products that can come out of this reaction.

Since the oxidating conditions that can foster the reaction are many, it was searched in the literature a case study that could be easily reproduced in the chemical lab, with moderate pressure conditions. This will be briefly exposed in this subparagraph.

The experiment found in literature and that was imitated is explained by Peter J. Miedziak and others. As reported in the following lines, they used another key reactant, glucose, and not HMF. Anyhow, it has been estimated that the same protocol could be transferred to the reaction of our interest, without significant changes, if not the obviously different range of products and subproducts potentially generated.

Typically to achieve high conversion of glucose into gluconic acid, a sacrificial base is added to the reaction and the pH of the solution is maintained by the continual addition of a base. All along the experiment, the same choice of the referring experience was made, i.e. Sodium hydroxide NaOH. (Peter Miedziak, 2014)

Diversely from the original procedure, pure oxygen has not been used as the oxidant. In fact, the preparation of oxygen from air, together with its purification, requires considerable energy which adds significantly to the cost of the process. Therefore, bubbling air through the solution was the source of the oxygen in our case.
The removal of the base from the process and its replacement with a catalytic equivalent, together with the utilization of air as a source of oxygen, would have represented a significant advance in the process for glucose oxidation adhering to the principles of green chemistry. Anyhow, we just limited to couple the effect of the reaction with our gold catalyst, but we opted to maintain the basic conditions during the reaction to enhance the power of the oxidant.

The solution of NP used was the red solution, which, containing smaller sized particles- as discussed in the paragraph concerning their characterization- was supposed to promise better performances.

Oxidation of glucose using air was carried out in a glass reactor consisting of a round-bottomed flask (50 ml) fitted with a reflux condenser. The gold catalyst (0.06 g) was suspended in the aqueous HMF solution (5 ml, 0.5 M HMF: the same molar concentration of the original study

was maintained but with HMF instead of glucose). The reacting mixture has been kept at 50 °C thanks to a heated pot placed on an electric plaque. The reaction mixture was stirred for 24h at atmospheric pressure. In the *photo 6.3* below, the schema of the process is shown:

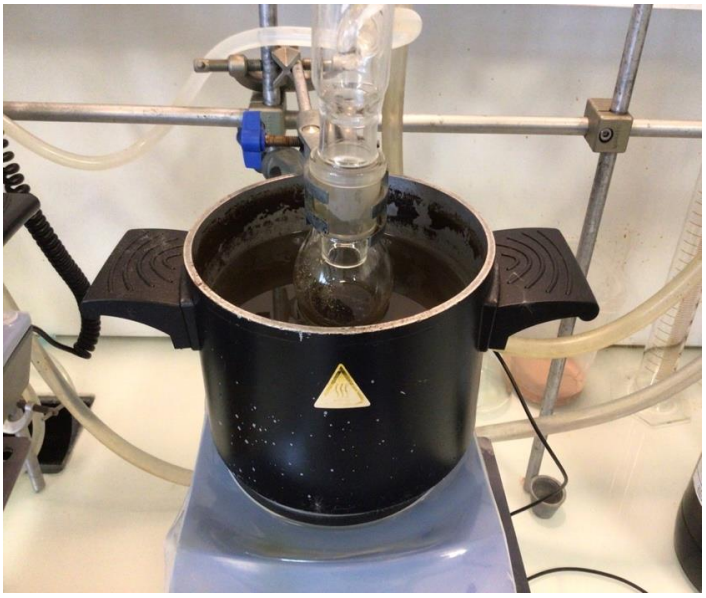

*Photo 6.3: Experimental apparatus for the chemical reaction*

Although the research team of Miedziak had conducted the reaction under mild condition to show that if a basic support is used the reaction can be carried out without the addition of the sacrificial base and PH control, in this case the PH was maintained to 9 by adding NaOH.

## 6.3 Analysis of the products

*Photo 6.4: vial containing the reacting mix after 24h*

Thin layer chromatography was conducted on a sample of the reacting mixture to study what had been going on during the 24h of reaction (see *Photo 6.4*).

Thin layer chromatography (TLC) is a chromatographic technique used to separate the components of a mixture using a thin stationary phase supported by an inert backing. In this case, its purpose is to be performed on the analytical scale as a mean of monitoring the progress of a reaction.
TLC functions on the same principle as all chromatography: a compound will have different affinities for the mobile and stationary phases, and this affects the speed at which it migrates. The discriminant of our test is the different polarity.

The targeted molecule we are interested in is furan-2,5-dicarboxylic acid (FDCA), visible in the scheme of the precedent paragraph. But, looking at that scheme, there's a broad spectrum of possible undesired subproducts that can be formed. They differ not only for their MW and degree of oxidation, but also for the functional group branched to the furanic ring, from which different polarities derive as well. An example of an intermediate molecule that could be obtained is 2,5-diformylfuran (DFF) or 5-hydroxymethyl-2-furancarboxylic acid (HMFCA), all visible in the *figure 6.5* underneath, taken from "Metal vs. Metal-Free Catalysts for Oxidation of 5- Hydroxymethylfurfural and Levoglucosenone to Biosourced Chemicals", (Erwann Guénin, 2022)**b**

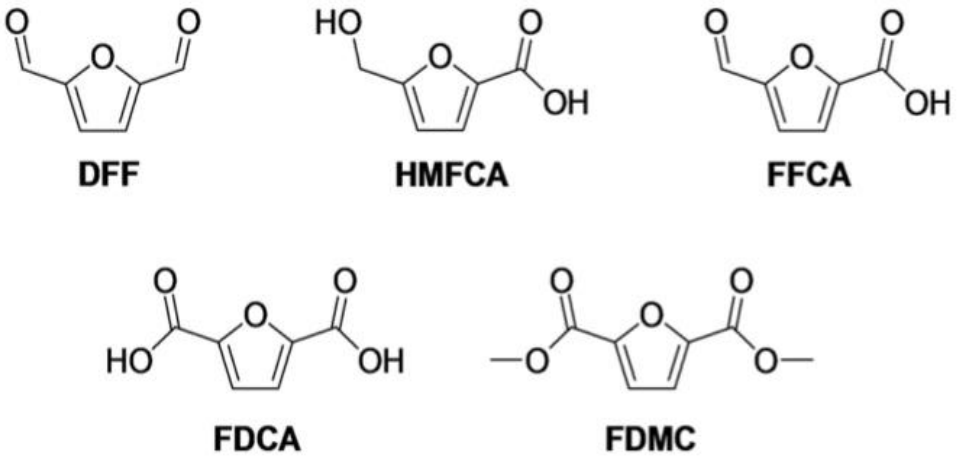


*Figure 6.5 Main products obtained from HMF oxidation by metal catalyst*

The goal is to exploit the difference in polarity due to the carboxylic function to distinguish these products, obtaining well defined, well separated spots.

TLC plates (also known as chromatoplates) made of silica gel constitute the stationary phases. The plates incorporate a compound which fluoresces under short-wave UV (254 nm). The backing of TLC plates is composed of glass. Glass plates are chemically inert and best withstand reactive stains and heat but are brittle and can be difficult to cut.

Therefore, a straight line was drawn to determine an adequate piece of layer and then this line was touched several times with the tip of a knife to cut it delicately.

The properties of the sample should be considered when selecting the stationary phase. Silica gel gives affinity with rather polar molecules, so it can be exclusively used for amino acids and hydrocarbons, with which it is able to interact via hydrogen bond's formation, as deducible by looking at figure 6.6, taken from Wikipedia with modifications. (Anon., s.d.)

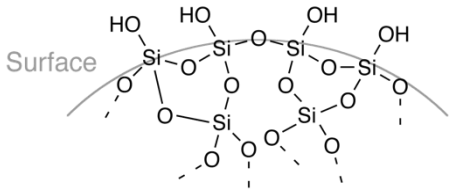


*Figure 6.6: Schematic representation of the silica surface*

Considering that the molecules belong to the family of the furan, this technical choice is reputed convenient for our case study.

Proper solvent selection is perhaps the most important aspect of TLC and determining the best solvent may require a degree of trial and error. As with plate selection, we need to keep in mind the chemical properties of the analytes. Normally, depending on the molecules to analyze, data can be sought in literature to guide the choice.

The starting solvent adopted was a mixture methanol:chloromethane with different ratios, the higher the percentage of methanol, the more the solvent becomes polar. After a separation is complete, individual compounds appear as spots separated vertically. Each spot has a retention factor (Rf) which is equal to the distance migrated over the total distance covered by the solvent.
Varying the ratio of the solvent mixture can have a pronounced effect on Rf. Values range from 0 to 1 with 0 indicating that the solvent polarity is very low and 1 indicating that the solvent polarity is very high. If the value is 0, you need to increase your solvent polarity because the sample is not moving and sticking to the stationary phase. If the value is 1, you need to decrease your solvent polarity because the compound was not able to separate.

The Rf value can be used to identify compounds due to their uniqueness to each compound. When comparing two different compounds under the same conditions, the compound with the larger Rf value is less polar because it does not stick to the stationary phase as long as the polar compound, which would have a lower Rf value. (Anon., 2022)

In our case different deposits of substances were effectuated on the bottom of the thin layer, all separated horizontally, as visible in the *photos 6.7 and 6.8*, and marked by a letter. This nomenclature will be adopted later on:

- M ➔ "mélange réactionnel", i.e. the reacted mixture whose composition is unknown
- R ➔ "réactif", i.e. the pure reactant HMF before undergoing any chemical reaction
- M+R ➔ a mixture of the two
- D ➔ referring to the desired product, FDCA

After that, the thin layer containing the deposits was placed vertically inside a beaker filled with the solvent below the marking line, so that by rising by capillarity the solvent would drag the samples all the way up the silica pores.
How fast the compounds travel up the plate depends on how much the compound is soluble in the solvent: it will travel further up the TLC plate if a perfect dissolution is obtained.

We were able to determine which firstly by looking at the Rf value, that can be seen by illuminating the plate with short-wave UV, and secondly by Quenching. *Photo 6.7,* visible below, shows the result of the migration by using a 20% MeOH solution as a solvent (left) and by using pure methanol (right).

First, it is necessary to interpretate the phenomenon that took place in the small layer containing only M and R (right side of *photo 6.7*). Visibly, as the presence of two big spots reveals, in M it is possible to identify two different substances with largely different $R_f$: one rather polar, who accumulated on the top of the layer, and the rest which got stuck close to the marking line, with less polar behavior. Instead, all the solute present in R crossed the entire length of the chromatoplate and stopped at the top, thus proving its affinity with the polar solvent. The hypothesis that we can make up with is that a chemical change must have happened during the reaction, otherwise the presence of compounds with different polarities in M would be unjustified. By observing the single, large spot above R, we can conclude that HMF has a good affinity with MeOH and it is responsible for the stain. By coupling these two pieces of information, we deduce that the molecule that is concentrated on top, above M must be the unreacted HMF. This hint tells us that the reaction reached an equilibrium with a yield <100%.

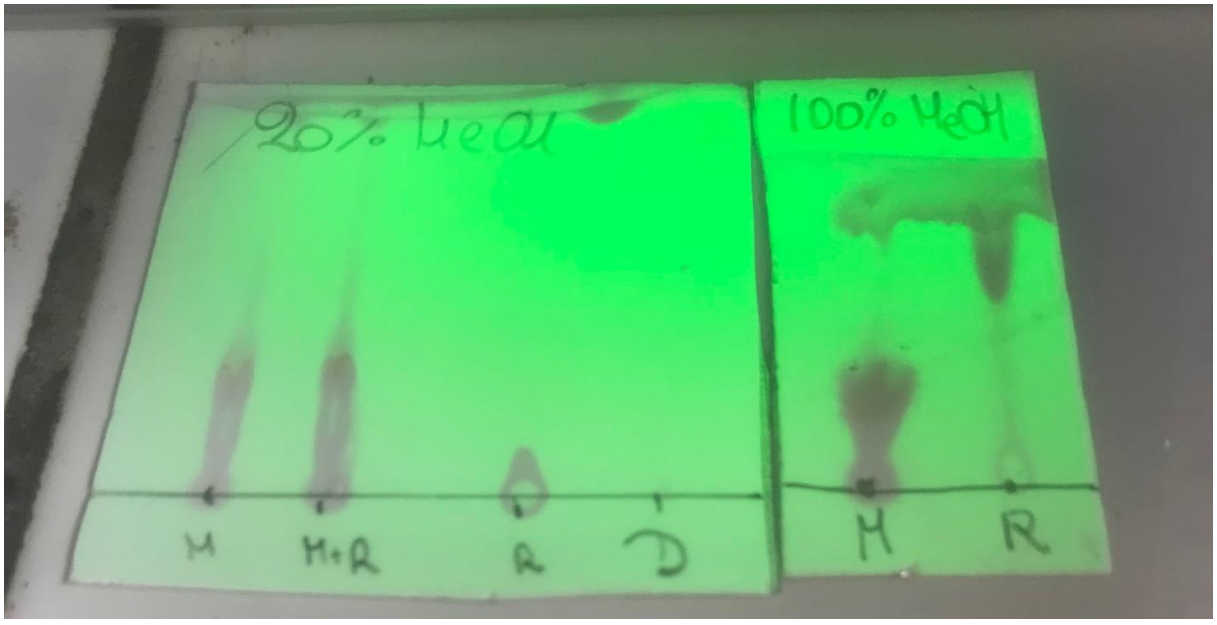


*Photo 6.7: Thin layer illuminated by UV light after migration of the samples*

Now we can focus on the left side of *photo 6.7,* where a broader gamma of deposits has been made. This time, since in the previous case the presence of $R_f$ =1 was observed, it was decided to attenuate the polarity of the solvent by setting a 20% of MeOH in chloromethane. The response of the compound observed is:

- D migrated to the top of the layer
- R kept its tendency to have very little displacement
- M spread over the lower half of the plate
- M+R showed the same behavior as just M

These hints provide us some more information: R and D with a medium-low polar solvent assume opposite behaviors, perhaps due to the additional carboxylic groups in D that allowed to better interact with the solvent. This fact only proves the different molecular structure of reactant and desired product, but it doesn't make us go further in the investigation of M.
Concerning the distribution of the compounds present in the mixtures M and M+R all over the plate, from a qualitative point of view they contain the same compounds, given the identical response. Moreover, it is possible to draw the hypothesis of the apparition of compound with intermediate properties between HMF and FDCA. This hypothesis withstands on the fact that if D was present in the mixture, it would have accumulated on top as pure D, but on the other hand, if HMF had not reacted at all, there would have been just one spot below as in R. Perhaps we witnessed to the formation of less oxygenated forms of HMF than the final FDCA, e.g. HMFA or DFF (all illustrated in the above mentioned f*igure 6.5*).

Unfortunately, from the engineering point of view, this result is the proof that the reaction failed in synthetizing the desired product. The reasons for this failure may lay on the efficacity of this type of catalysis and it is excluded that are linked neither to the cautiously long reaction time nor to the pushed basic pH. Only comparison with the hybrid catalysis will give an answer to this dilemma.

Quenching causes dark spots on the surface of the plate. The *photo 6.8* shows the result after making an oxidation test with $KMnO_4$. To develop a plate with permanganate, the plate was dipped inside a jar containing $KMnO_4$ and heated with a heat-gun until yellow/brown spots appeared.

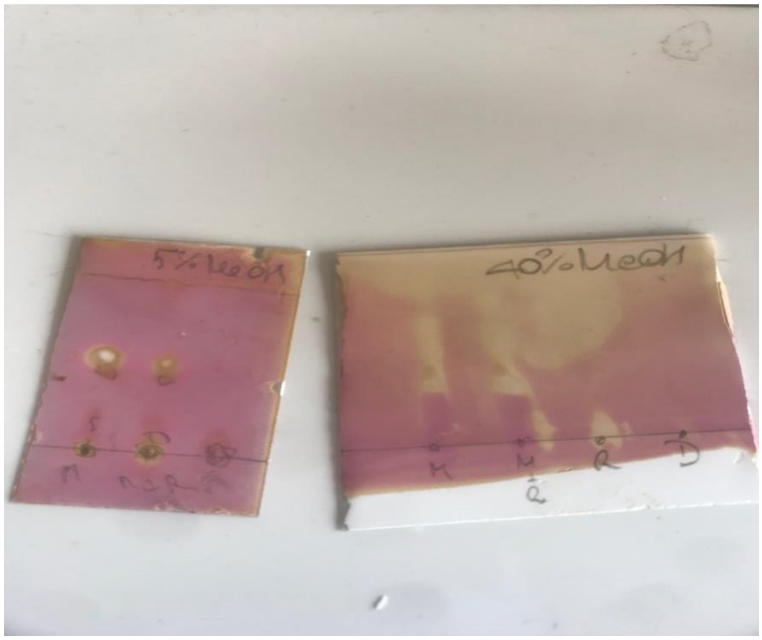

*Photo 6.8: Chromatoplates after immersion in $KMnO_4$ jar with visible spots*

# 7. Overall conclusions

The experimental work conducted at UTC laboratories accompanied by the literature search summarized so far was aimed at the synthesis of a hybrid catalyst for the oxidation and functionalization of furan molecules derived from biomass.
However, each individual part of the experiments has its own individual utility; therefore, it is possible to identify alongside the general objective that directed the research, giving it its organicity, a series of 'tasks' that were explored to achieve it.
These include: the synthesis and characterization of gold nanoparticles, the extraction of fibroin from silk, its gelation, and the HMF oxidation test.
These micro-areas of scientific interest have allowed us to reap rewards in an absolute sense.

The formation of metal nanoparticles was undoubtedly the most fervid part of the experience. Thanks to the synthesis with the microwave reactor, a homogeneous dispersion of particles of the desired size, around 20 nm in diameter, was obtained; this success due to the synthesis route carried out by Aufare, allows us to endorse his substantial modifications from Turkevich's previous synthesis.
Analytical techniques to characterize dispersion are doubly useful: both for the intrinsic qualitative and for quantitative inspection of nanoparticles and to make me approach the sophisticated laboratory devices used to conduct them. Although for each microscopic analysis there was a professional operator responsible for conducting it, I underwent specific training in order to understand the principle of operation of the apparatus and correctly interpret the results.

The hardest section of the work was the extraction of fibroin. Although the applied procedure had already been tested, several variables can intervene in the process in each step, invalidating the result and making it necessary to start over, as discussed in section 4.3 “Troubleshoots”. Given the satisfactory quality of solution obtained by following the Rockwood protocol, it can be concluded that it is one of the best in the current panorama; however, the practice carried out and especially the numerous incidents encountered allow for some improvements attempted to be summarized below.
The duration of the degumming phase can be increased by 10 minutes; due to this additional time, the cocoons now deprived of sericin have a chance to intertwine into a single fibroin pad, and the aqueous phase will also acquire a more turbid coloration, indicative of the increase in concentration of sericin transferring into the solvent.
When injecting fibroin into dialysis cassettes, it is advisable to add distilled water to fluidize the solution; in fact, as it cools during the process, its viscosity will tend to increase, making it more difficult to flow through the syringe bore. This amount of water should be measured and taken into account when calculating the fibroin concentration of the solution and should not be such that this value falls below 4%.
The dialysis step constitutes the litmus test of the procedure: it is at this stage that it will be seen whether the process will bear fruit, or the solution is defective.
During experimental practice, given the abundant amount of fibroin needed to fabricate the hydrogels, this step was repeated eight times, but only two of the eight times was the result adequate. The main failures resulted in the solidification of the solution once the removed LiBr could no longer prevent the proteins from re-aggregating. One strategy to overcome this problem is to decrease the dialysis time slightly, constantly monitoring the consistency of the

fibroin in solution, and stop it if it began to thicken, but not by more than a day: too much decrease will make the time insufficient to remove all the LiBr present.
Another aspect not to be underestimated is the rate at which fibroin, now isolated and dissolved in pure solution, can re-aggregate and gel before the addition of the appropriate enzymes. There can be many causes, such as bumps between particles caused during centrifugation and inadvertently shaking the vial containing the solution in handling it.
In any case, the time factor always plays a negative role, so it is advisable to subject the solution to the gelling protocol immediately, before it does so spontaneously.

Once the fibroin was extracted, the two protocols to initiate gelation by enzyme, both the one with HRP and the one with laccase, reported in Section 5.2, were implemented. Experimental reality showed that only the second one provided good results.
Using the protocol with HRP, in fact, the fibroin solution did not assume a gelatinous morphology, remaining in a liquid state inside the silicone mold. It is not immediate to conclude whether it was the fault of the quality of the previously obtained fibroin or rather of its implementation; further attempts may provide more reliable statistical data to hypothesize a better efficacy of one enzyme over the other; however, since upstream the fibroin extraction protocol worked only twice, it was not possible to repeat the practice more than once for each enzyme.

The research concluded with the test of HMF oxidation by atmospheric oxygen catalyzed by gold in the form of nanoparticles solution, following the protocol already existing in the literature, adapted to the precipitated purpose of the investigation. The results obtained by chromatographic analysis detailed in Section 6.3 highlight that the oxidation, although not in unity yield, as evidenced by the presence of unreacted HMF in the reaction mixture, took place in the dedicated reaction time; however, the product obtained, shows a behavior on chromatographic examination halfway between the HMF reagent and the desired FDCA product, indicating the possible formation of a by-product with an intermediate oxidation state, such as FDF or HMFA. Only NMR analysis could help to discern between the hypotheses.

The processes applied in these areas can be consulted for those who will soon try their hand at this research in order to comfort their results, but also to continue it; in fact, the final stage of the work, in which the obtained nanoparticles are grafted into the silk hydrogel to obtain the hybrid catalyst, remains to be explored.
An interesting aspect will be to observe the interaction of the nanoparticles and the gelling mechanism, operating an appropriate rheological test if that is the case.
After performing the same test on the oxidation of HMF with a protocol adapted to the new catalyst, it will be possible to compare the performances of the two models: on the one hand to study the range of products obtained by thin-layer chromatography or other more refined analytical techniques such as NMR or IR spectroscopy, and on the other hand to compare the reaction times and yield.

# 8. Acknowledgements

*Mi è doveroso dedicare questo spazio del mio elaborato alle persone che hanno contribuito con il loro supporto alla realizzazione dello stesso.*
*Ringrazio quindi la mia relatrice, Professoressa Stefania Specchia, per la pazienza mostratami e per i suoi suggerimenti dispensati durante tutto il percorso di stesura dell'elaborato.*
*Inoltre, le sono grato di essere stata la mia referente italiana durante il mio scambio in Francia; questa esperienza ha determinato irreversibilmente una svolta nella mia vita.*
*Per l'indomito entusiasmo trasmessomi nella scelta della meta, Compiègne, dove si è svolto il mio Erasmus, ringrazio Matteo. I tuoi consigli sono stati preziosi.*

*Sono grato ai miei genitori che mi hanno congiuntamente sostenuto fin dal principio del mio percorso di studi. A mio padre per le sue concrete premure nei miei confronti e a mia Madre per le delicate attenzioni che mi ha dedicato (anche quando diventavano ammorbanti).*
*Voglio anche esprimere la mia gratitudine a mia sorella maggiore, che rimarrà sempre tale ai miei occhi, anche se adesso crede di avere una famiglia tutta sua. Sono io numero zero.*

*In questo momento il mio pensiero va a quelle persone con cui ho condiviso tutto il mio percorso universitario, seppur non tra le schiere di banchi del Politecnico e nella diversità delle nostre scelte accademiche … Con loro la distanza scompare in un attimo, e sapremo sempre ritrovarci nella nostra isola natia.*

*J'ai le plaisir de remercier même une amie dont l'aide a été indispensable pour bien réussir à trouver la bonne route vers mon futur. Merci Sholah pour ta patience, ton impédance, que tu m'as démontré à maintes reprises au pic avec mes candidatures pour les écoles doctorales !*

## 9. List of abbreviations

NP = nanoparticles

HMBP = 1-hydroxy-1,1-méthylène bisphosphonate
HMBP_Bn = 1-hydroxy-1-phenyl bisphosphonate
HMBP_= = 1-hydroxy-1- phosphonopent-4-ynyl phosphonate

HMF = 5-hydroxymethyl furfural
HMFCA = 5-hydroxymethyl-2-furancarboxylic acid
DFF = 2,5-diformylfuran
FDCA = furan-2,5-dicarboxylic acid

SF = silk fibroin
SS = silk sericin
MW = molecular weight

TEM = transmission electronic microscopy
SEM = scansion electronic microscopy
DLS = Dynamic light scattering
MWCO = molecular weight cut out

MCO = multi copper oxidase
HRP = The enzyme horseradish peroxidase

TLC = Thin layer chromatography
Rf = Retention factor

# 10. List of sources


Anon., 2022. [Online]
Available at: https://www.sigmaaldrich.com/IT/it/technical-documents/technical-article/analytical-chemistry/green-chemistry-principles
Anon., 2022. [Online]
Available at: http://www.fibroinadiseta.it/cose-fibroina-seta/
[Accessed 09 17 2022].
Anon., 2022. *Libre Texts.* [Online]
Available at:
https://chem.libretexts.org/Ancillary_Materials/Demos_Techniques_and_Experiments/General_Lab_Techniques/Thin_Layer_Chromatography
[Accessed 10 09 2022].
Anon., 2022. *Merck.* [Online]
Available at: https://www.sigmaaldrich.com/IT/it/technical-documents/technical-article/analytical-chemistry/green-chemistry-principles
[Accessed 22 08 2022].
Anon., 2022. *Merck.* [Online]
Available at: https://www.sigmaaldrich.com/IT/it/technical-documents/technical-article/analytical-chemistry/green-chemistry-principles
[Accessed 08 08 2022].
Anon., 2022. *Royal society of Chemistry.* [Online]
Available at: https://www.rsc.org/periodic-table/element/79/gold
[Accessed 14 06 2022].
Anon., 2022. *Technology networks.* [Online]
Available at: https://www.technologynetworks.com/analysis/articles/sem-vs-tem-331262
[Accessed 23 07 2022].
Anon., 2022. *uIowa.* [Online]
Available at: https://cmrf.research.uiowa.edu/transmission-electron-microscopy
[Accessed 23 07 2022].
Anon., 2022. *Wikipedia.* [Online]
Available at: https://en.wikipedia.org/wiki/Einstein_relation_(kinetic_theory)#Stokes–Einstein_equation
[Accessed 23 08 2022].
Anon., 2022. *Wikipedia.* [Online]
Available at: https://en.wikipedia.org/wiki/Horseradish_peroxidase
[Accessed 1 09 2022].
Anon., n.d. [Online]
Available at: https://www.sigmaaldrich.com/IT/it/technical-documents/technical-article/analytical-chemistry/green-chemistry-principles
Anon., n.d. *Dynamic biosensors.* [Online]
Available at: https://www.dynamic-biosensors.com/ufaqs/how-is-the-hydrodynamic-diameter-defined/
[Accessed 21 08 2022].

Anon., n.d. *Wikipedia.* [Online]
Available at:
https://upload.wikimedia.org/wikipedia/commons/b/b5/Schematic_silica_gel_surface.png
[Accessed 4 09 2022].
Aufare, R., 2016. *Synthèse et fonctionnalisation de nanoparticules d'or à l'aide de molécules phosphorées,* Paris: s.n.
Aufare, R., 2018. *Synthèse et fonctionnalisation de nanoparticules d'or à l'aide de molécules phosphorées,* Paris: Journal RSC Adv.
Basu, P. B. e. A., 2015. Advanced testing of silk fibers, yarns, and fabrics. *Advances in Silk Science and Technology.*
Begher, I., 2022. *La Terlaina.* [Online]
Available at: https://terlaina.pgzaltopianovigolana.it/2022/03/09/bombyx-mori-che-cose/
[Accessed 11 09 2022].
Carter, D. W. a. B., 1996. Transmission electron microscopy. In: s.l.:Plenum, pp. 3-17.
Cerini, S., n.d. *UniBo.* [Online]
Available at: https://chimica-industriale.unibo.it/it/terza-missione/impresa/consulenze-e-prestazioni/dynamic-light-scattering-dls
[Accessed 21 08 2022].
Cristina Belda Marín, C. E. V. H. Y. L. L. M. J. L. a. E. G., 2021. Gold, Silver, and Iron Oxide Nanoparticle Incorporation into Silk Hydrogels for Biomedical Applications: Elaboration, Structure, and Properties. *ACS Biomaterials Science and Enginnering,* p. 1.
Danielle Rockwood, R. P. T. Y. X. W. M. L. &. D. K., 2011. Materials fabrication from Bombyx mori silk fibroin.
Dauphin, Y., 2021. *Synthèse de nanoparticules métalliques pour des applications en photothérapie,* Compiègne: s.n.
Erik van der Linden, E. A. F., 2009. Gelation: Priciples, Models and Applications to Proteins.
Erwann Guénin, G. E. N. A. J. T., 2022. Metal vs Metal-Free Catalysts for Oxidation of 5-Hydroxymethylfurfural and Levuglucosenone to Biosourced Chemicals. *ChemsusChem,* Issue doi.org/10.1002/cssc.202102606, pp. 1-25.
Francesco Nocito, M. V. M. A. e. A. D., 2022. Selective oxidation of HMF to DFF Using Water as Solvent and Oxygeb as Oxidant with Earth-Crust-Abundant Mixed Oxides. *National center for Biotechnology Information.*
Hermanson, G. T., 2013. Enzyme Modification and Conjugation. In: *Bioconjucate Techniques.* s.l.:s.n.
Hirsch, P., 1965. Electron microscopy of thin crystals. In: s.l.:Butterworths.
J. Bello, H. B., 1961. Interaction of Model Peptides with Water and Lithium Bromide. *Nature,* pp. 440-441.
Jimmy Law, A. B., 2022. *Libre Texts Chemistry.* [Online]
Available at:
https://chem.libretexts.org/Bookshelves/Physical_and_Theoretical_Chemistry_Textbook_Maps/Supplemental_Modules_(Physical_and_Theoretical_Chemistry)/Physical_Properties_of_Matter/Solutions_and_Mixtures/Colloid
[Accessed 10 08 2022].
Kustov, 2021. Catalysis by Hybrid Nanomaterials.
Kustov, 2021. Catalysis by Hybrid Nanomaterials. *Molecules.*
Lancashire, R., 2011. *UWI-Mona.* [Online]
Available at:

http://wwwchem.uwimona.edu.jm/courses/CHEM2402/Textiles/Animal_Fibres.html
[Accessed 13 06 2022].
Lee, A., n.d. *Big Rock Exploration.* [Online]
Available at: https://bigrockexploration.com/2020/06/crystallography-of-gold/
[Accessed 11 06 2022].
Lewis, M., 1996. Solid rheology and texture. In: *Physical Properties of Foods and Food Processing Systems.* s.l.:s.n.
M. Tuomela, A. H., 2011. Environmental Biotechnology and Safety. In: *Comprehensive Biotechnology.* s.l.:s.n.
Marin, C. B., 2021. Gold, Silver, and iron Oxide Nanoparticle Incorporation into Silk Hydrogels for Biomedical Apllications.
N.A. Peppas, B. S. M. K., 2012. Hydrogels. In: Elsevier, ed. *Polymer Science: A Comprehensuive Reference.* s.l.:Krzysztof Matyjaszewski, Martin Möller, pp. 385-395.
Nadim Ayoub, J. T. E. G. a. G. E., 2022. Metal vs. Metal-Free Catalysts for Oxidation of 5-Hydroxymethylfurfural and Levoglucosenone to Biosourced Chemicals. *ChemSusChem,* p. 1.
Nadim Ayoub, J. T. E. G. G. E., 2022. Metal vs. Metal-Free Catalysts for Oxidation of 5-Hydroxymethylfurfural and Levoglucosenone to Biosourced Chemicals. *ChemSusChem,* p. 4.
National center for Biology Information, 2022. *PubChem.* [Online]
Available at: https://pubchem.ncbi.nlm.nih.gov/compound/5-Hydroxymethylfurfural
[Accessed 11 08 2022].
Park, K. H., 2021. *MDPI.* [Online]
Available at: https://www.mdpi.com/journal/catalysts/special_issues/Hybrid_Catalysis
[Accessed 08 08 2022].
Paul Anastas, J. W., 1998. Green Chemistry Theory and Practice. *Oxford University Press: New York.*
Peter Miedziak, H. A. S. K. T. C. T. D. M. M. D. M. D. W. D. K. S. T. G. H., 2014. Base-free glucose oxidation using air with supported gold catalysts. *Green Chem,* Issue 16, 3132.
Petrucci, 2007. In: U. S. River, ed. *General Chemistry: Principles & Modern Applications.* New Jersey: s.n.
Priyadarshi, K. S. P. P. E. D. T., 2021. Mechanisms of ultrasonic de-agglomeration of oxides through in-situ high-speed observations and acoustic measurements. pp. 1-12.
Rei, C., 2021. *Développement d'un bioprocédé de dépollution des eaux et de valorisation de la biomasse,* Compiègne: s.n.
Shengshui Hu, Y. X., 2008. Biosensors based on direct electron transfer of protein. In: *Electrochemical Sensors, Biosensors and their Biomedical Applications.* s.l.:s.n.
Sophie Allart, A. C., n.d. *Manuel d'analyse d'images avec le logiciel ImageJ,* s.l.: s.n.
Tognon, G., 2022. *Papilionea.* [Online]
Available at: https://www.papilionea.it/bombyx-mori/
[Accessed 12 09 2022].